Recent advances in the analysis of biomagnetic signals

Kensuke Sekihara

Mind Articulation Project, Japan Science and Technology Corporation

Tokyo Metropolitan Institute of Technology

Application of spatial filter techniques to biomagnetic source localization

Definitions

- data vector: $\boldsymbol{b}(\mathrm{t}) = \begin{bmatrix} b_1(t) \\ b_2(t) \\ \vdots \\ b_M(t) \end{bmatrix}$

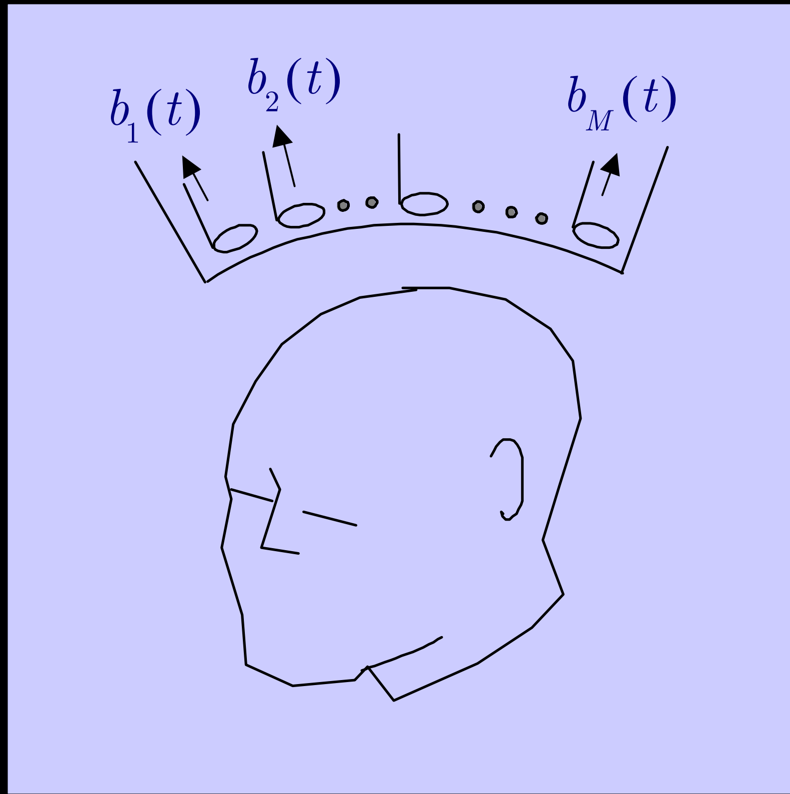

$\left[b_j(t) \text{: the } j\text{th sensor recording at } t \right]$

- data covariance matrix: $\boldsymbol{D} = \left\langle \boldsymbol{b}(t)\boldsymbol{b}^T(t) \right\rangle$

$\langle \cdot \rangle$ represents time average

Source moment

- magnitude at $\boldsymbol{r} = [x, y, z]$

  and at t: $s(\boldsymbol{r}, t)$

- orientation:

$$h(\boldsymbol{r}, t) = [h_x(\boldsymbol{r}, t), h_y(\boldsymbol{r}, t), h_z(\boldsymbol{r}, t)]$$

- source moment vector:

$$\boldsymbol{s}(\boldsymbol{r}, t) = s(\boldsymbol{r}, t) \begin{bmatrix} \boldsymbol{h}_x(\boldsymbol{r}, t) \\ \boldsymbol{h}_y(\boldsymbol{r}, t) \\ \boldsymbol{h}_z(\boldsymbol{r}, t) \end{bmatrix} = \begin{bmatrix} s_x(\boldsymbol{r}, t) \\ s_y(\boldsymbol{r}, t) \\ s_z(\boldsymbol{r}, t) \end{bmatrix}$$

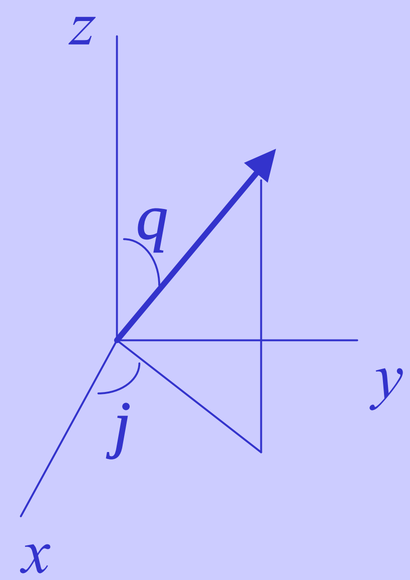

$$\boldsymbol{h}_x = \sin \boldsymbol{q} \cos \boldsymbol{j}$$

$$\boldsymbol{h}_y = \sin \boldsymbol{q} \sin \boldsymbol{j}$$

$$\boldsymbol{h}_x = \cos \boldsymbol{q}$$

Lead field vector for the j th sensor

$$\boldsymbol{l}_j(\boldsymbol{r}) = [l_j^x(\boldsymbol{r}),\ l_j^y(\boldsymbol{r}),\ l_j^z(\boldsymbol{r})]$$

Lead field matrix for the whole sensor array

$$\boldsymbol{L}(\boldsymbol{r}) = \begin{bmatrix} \boldsymbol{l}_1(\boldsymbol{r}) \\ \boldsymbol{l}_2(\boldsymbol{r}) \\ \vdots \\ \boldsymbol{l}_M(\boldsymbol{r}) \end{bmatrix} = \begin{bmatrix} l_1^x(\boldsymbol{r}) & l_1^y(\boldsymbol{r}) & l_1^z(\boldsymbol{r}) \\ l_2^x(\boldsymbol{r}) & l_2^y(\boldsymbol{r}) & l_2^z(\boldsymbol{r}) \\ \vdots & \vdots & \vdots \\ l_M^x(\boldsymbol{r}) & l_M^y(\boldsymbol{r}) & l_M^z(\boldsymbol{r}) \end{bmatrix}$$

Basic relationship

$$b_j(t) = \int \boldsymbol{l}_j(\boldsymbol{r})\boldsymbol{s}(\boldsymbol{r},t)\,d\boldsymbol{r}$$

or

$$\boldsymbol{b}(t) = \int \boldsymbol{L}(\boldsymbol{r})\boldsymbol{s}(\boldsymbol{r},t)\,d\boldsymbol{r}$$

Problem of source localization:

Estimate $\boldsymbol{s}(\boldsymbol{r},t)$ from the measurement $\boldsymbol{b}(t)$

Spatial filter

$$\hat{\boldsymbol{s}}(\boldsymbol{r},t) = \boldsymbol{w}^T(\boldsymbol{r})\boldsymbol{b}(t) = [w_1(\boldsymbol{r}),\ldots,w_M(\boldsymbol{r})]\begin{bmatrix} b_1(t) \\ \vdots \\ b_M(t) \end{bmatrix}$$

⇑ estimate of $\boldsymbol{s}(\boldsymbol{r},t)$

⇑ weight vector

(neglecting the explicit time notation)

$$\left.\begin{aligned} \boldsymbol{b} &= \int \boldsymbol{L}(\boldsymbol{r})\boldsymbol{s}(\boldsymbol{r})\,d\boldsymbol{r} \\ \hat{\boldsymbol{s}}(\boldsymbol{r}) &= \boldsymbol{w}^T(\boldsymbol{r})\boldsymbol{b} \end{aligned}\right\} \rightarrow \hat{\boldsymbol{s}}(\boldsymbol{r}) = \int \underbrace{\boldsymbol{w}^T(\boldsymbol{r})\boldsymbol{L}(\boldsymbol{r}')}_{\mathbb{R}(\boldsymbol{r},\boldsymbol{r}')}\boldsymbol{s}(\boldsymbol{r}')\,d\boldsymbol{r}'$$

Resolution kernel → $\mathbb{R}(\boldsymbol{r},\boldsymbol{r}')$

Resolution kernel: $\hat{s}(\boldsymbol{r}) = \int \mathbb{R}(\boldsymbol{r}, \boldsymbol{r}')\boldsymbol{s}(\boldsymbol{r}')d\boldsymbol{r}'$

The weight $\boldsymbol{w}(\boldsymbol{r})$ must be chosen so that the resolution kernel has a reasonable shape.

What is reasonable shape?

- peak at $\boldsymbol{r}$
- small mail-lobe width
- low side-lobe amplitude

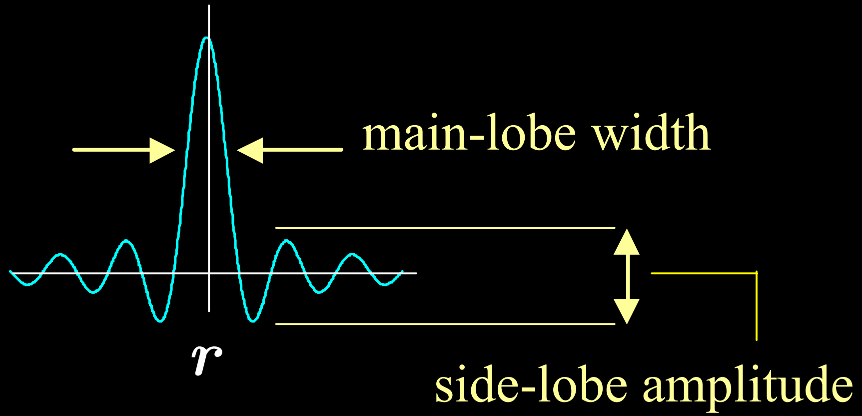

Non-adaptive weight

$w(r)$ is data independent

Adaptive weight

$w(r)$ is data dependent

Data-independent (non-adaptive) weight

- Spatial resolution is limited by sensor-array configuration.
- Final results are not influenced by source temporal correlation.

Data-dependent (adaptive) weight

- Spatial resolution can exceed the limit imposed by the sensor-array configuration.
- Strong temporal correlation among source activities severely degrade the quality of final estimation results

Data-independent (non-adaptive) weight

minimum-norm estimate (Hamalainen *et al.*)

The weight $\boldsymbol{w}(\boldsymbol{r})$ is obtained by

$$\min \int \left[\mathbb{R}(\boldsymbol{r}, \boldsymbol{r}') - \boldsymbol{d}(\boldsymbol{r} - \boldsymbol{r}') \right]^2 d\boldsymbol{r}'$$

$$\Downarrow$$

$$\boldsymbol{w}^T(\boldsymbol{r}) = \boldsymbol{L}^T(\boldsymbol{r})\boldsymbol{G}^{-1}, \text{ where } G_{i,j} = \int \boldsymbol{l}_i(\boldsymbol{r})\boldsymbol{l}_j(\boldsymbol{r})d\boldsymbol{r}$$

Inverse solution: $\hat{\boldsymbol{s}}(\boldsymbol{r}) = \boldsymbol{L}^T(\boldsymbol{r})\boldsymbol{G}^{-1}\boldsymbol{b}$

Property of *G* matrix

$$G_{i,j} = \int \boldsymbol{l}_i(\boldsymbol{r})\boldsymbol{l}_j(\boldsymbol{r})d\boldsymbol{r}$$

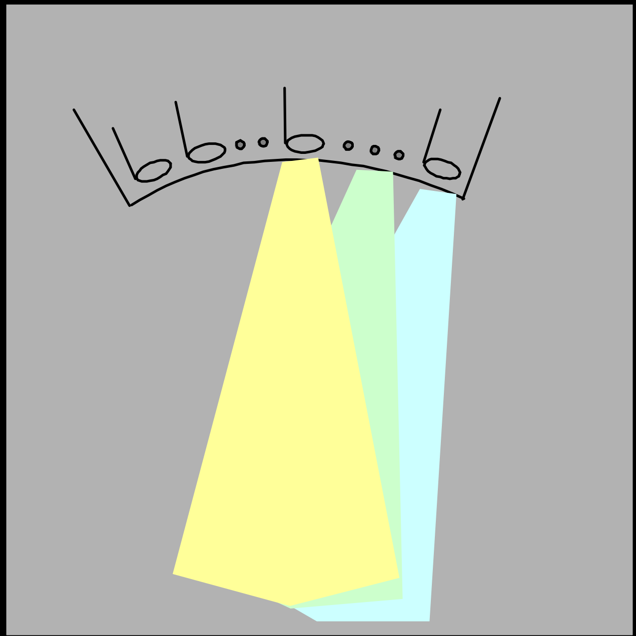

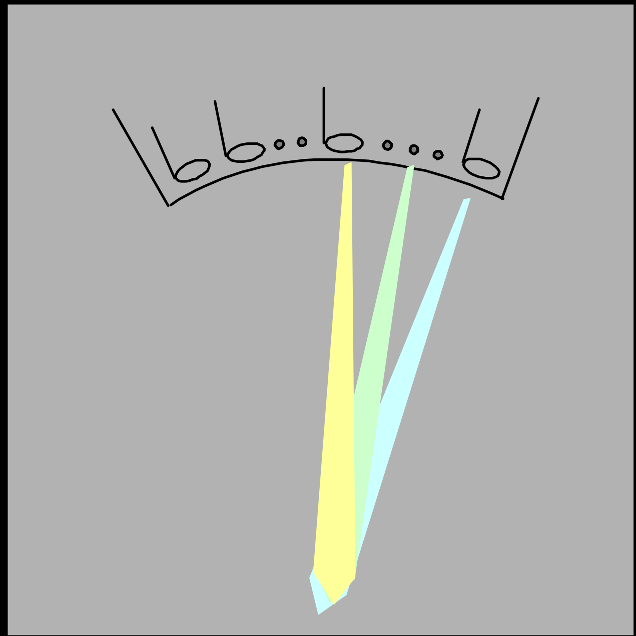

Overlaps of sensor lead fields is large

G is poorly conditioned

Overlaps of sensor lead fields is small

G has a small condition number

$\boldsymbol{G}$ is usually calculated by introducing pixel grid $\boldsymbol{r}_j$

$$b = \int \boldsymbol{L}(\boldsymbol{r})\boldsymbol{s}(\boldsymbol{r})\,d\boldsymbol{r} = \sum_{j=1}^{N} \boldsymbol{L}(\boldsymbol{r}_j)\boldsymbol{s}(\boldsymbol{r}_j)$$

$$= \underbrace{\left[\boldsymbol{L}(\boldsymbol{r}_1), \quad \cdots, \quad \boldsymbol{L}(\boldsymbol{r}_N)\right]}_{\boldsymbol{L}_N} \underbrace{\begin{bmatrix} \boldsymbol{s}(\boldsymbol{r}_1) \\ \vdots \\ \boldsymbol{s}(\boldsymbol{r}_N) \end{bmatrix}}_{\boldsymbol{s}_N} = \boldsymbol{L}_N \boldsymbol{s}_N$$

Therefore $\boldsymbol{G} = \boldsymbol{L}_N \boldsymbol{L}_N^T$ and

$$\boldsymbol{w}^T(\boldsymbol{r}) = \boldsymbol{L}^T(\boldsymbol{r})(\boldsymbol{L}_N \boldsymbol{L}_N^T)^{-1}$$

or

$$\boldsymbol{w}^T(\boldsymbol{r}) = \boldsymbol{L}^T(\boldsymbol{r})(\boldsymbol{L}_N \boldsymbol{L}_N^T + g\,\boldsymbol{I})^{-1}$$ [regularized version]

Minimum-norm weight with normalized lead field

$$\boldsymbol{w}(\boldsymbol{r}) = (\bar{\boldsymbol{L}}_N^T \bar{\boldsymbol{L}}_N + g\,\boldsymbol{I})^{-1} \boldsymbol{L}(\boldsymbol{r}) / \|\boldsymbol{L}(\boldsymbol{r})\|$$

where $\bar{\boldsymbol{L}}_N = \left[\frac{\boldsymbol{L}(\boldsymbol{r}_1)}{\|\boldsymbol{L}(\boldsymbol{r}_1)\|}, \quad \cdots, \quad \frac{\boldsymbol{L}(\boldsymbol{r}_N)}{\|\boldsymbol{L}(\boldsymbol{r}_N)\|} \right]$

Minimum-norm estimate with normalized weight

Calculate $\hat{q}(\boldsymbol{r}) = \left\|\boldsymbol{w}^T(\boldsymbol{r})\boldsymbol{b}\right\|^2 / \left\|\boldsymbol{w}(\boldsymbol{r})\right\|^2$

Dale *et al.*,
Valdes *et al.*

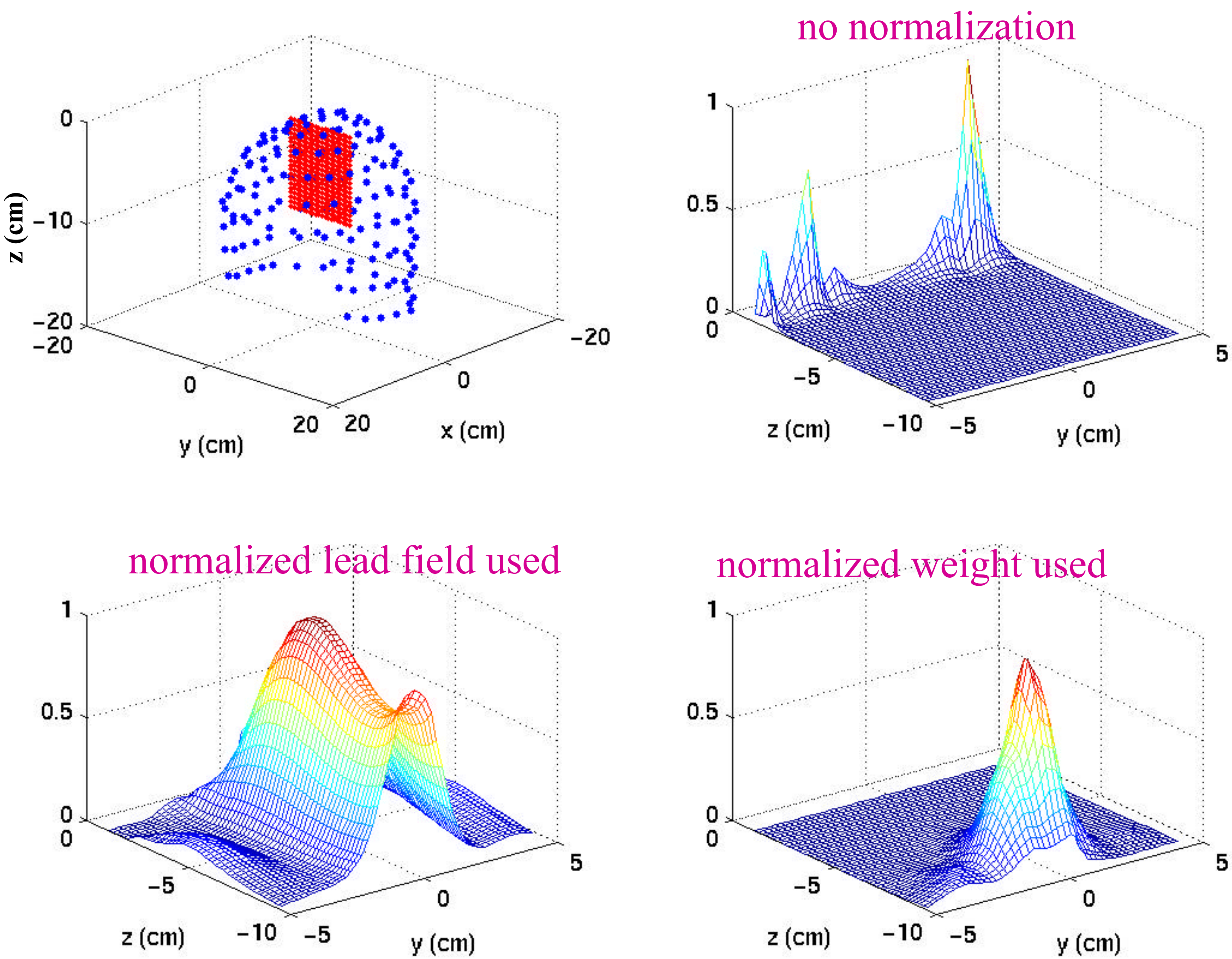

no normalization
normalized lead field used
normalized weight used
z (cm)
y (cm)
x (cm)
0
-10
-20
20
-5
5
0.5
1

Source imaging experiments

- Auditory-evoked field were measured using 148-channel whole-head sensor array (Magnes 2500).

Stimulus: 1-kHz pure tone applied to subject's left ear
Data acquisition: 1 kHz sampling frequency, 1-400 Hz bandpass filtering, 100 epochs averaged

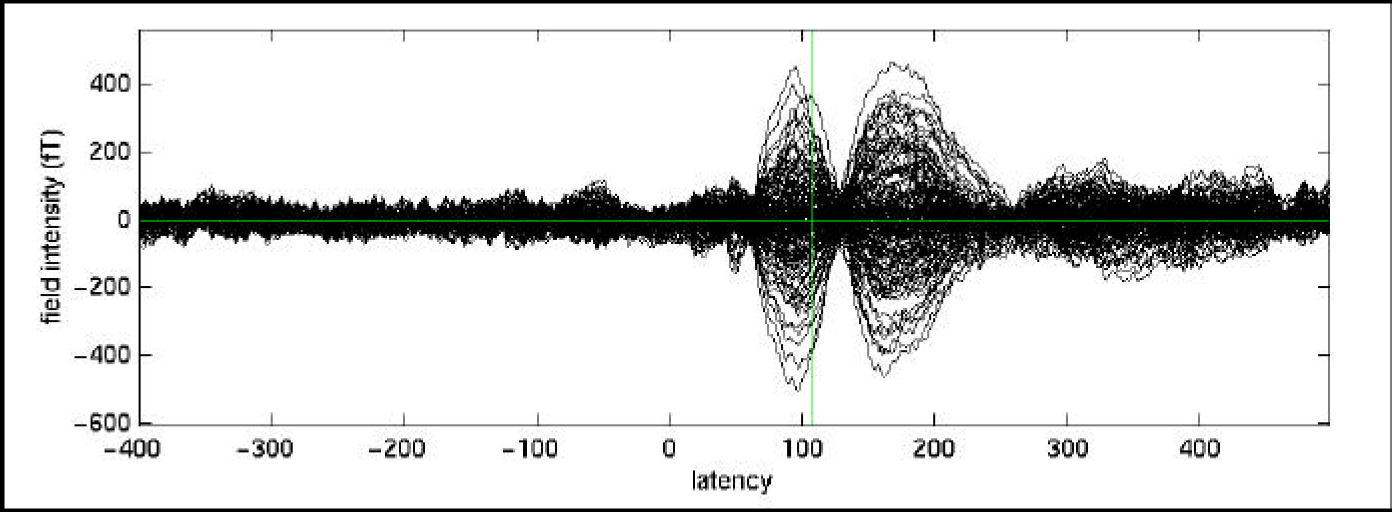

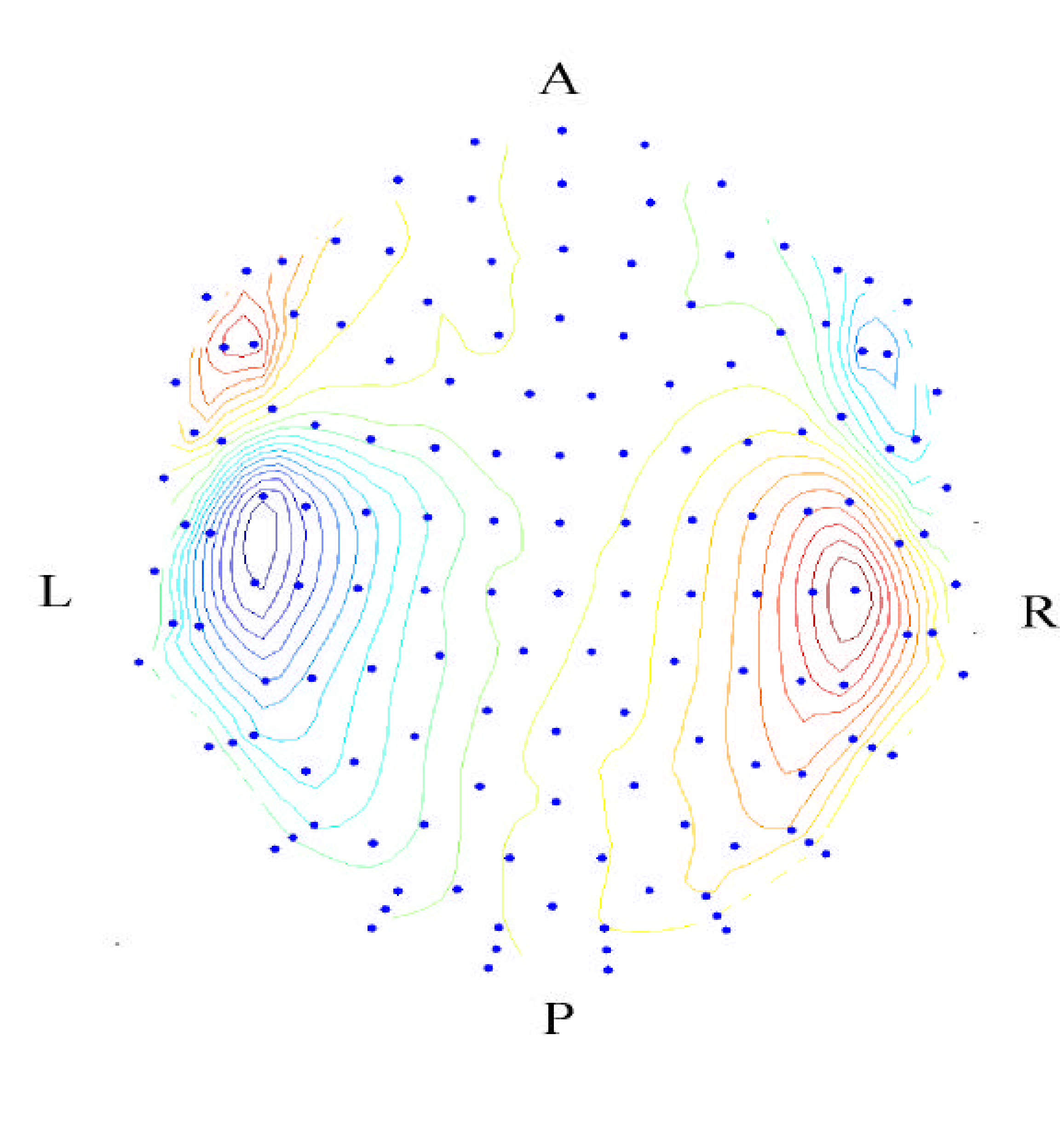
A
L
R
P

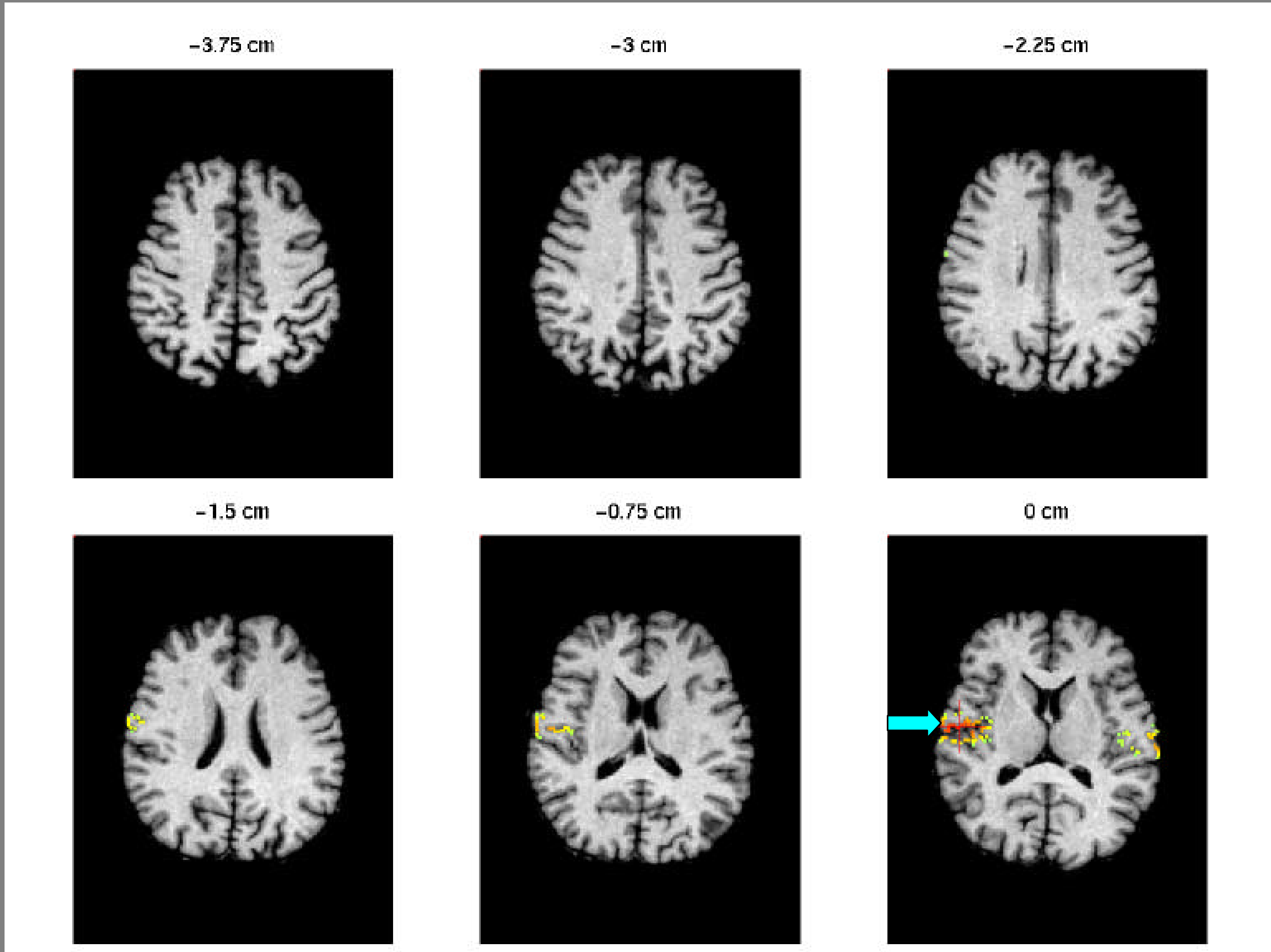
-3.75 cm
-3 cm
-2.25 cm
-1.5 cm
-0.75 cm
0 cm

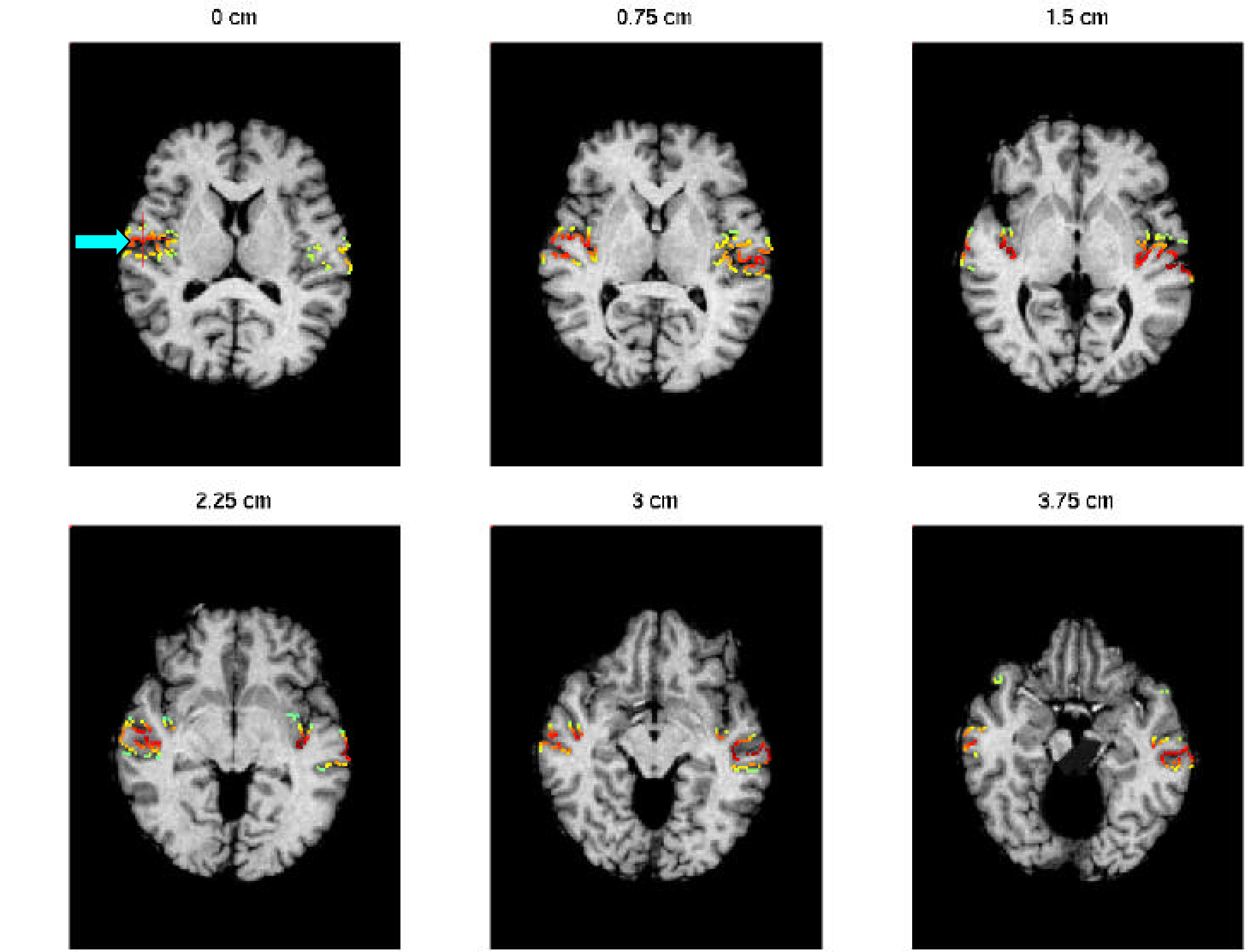
0 cm
0.75 cm
1.5 cm
2.25 cm
3 cm
3.75 cm

Linear-estimation-based methods

•LORETTA: impose the maximum-smoothness constraint. (Pascual-Marqui *et al*.)

•fMRI constraint: constrain solution based on fMRI results. (Dale *et al*.)

•FOCUSS: obtain a focal solution iteratively. (Gorodnitsky *et al*.)

•Bayesian approach: impose prior assumptions. (Schmidt *et al*.)

•l_1-norm approach: use the l_1-norm, instead of using the l_2-norm. (Matuura *et al*., Uutela *et al*., Beucker *et al.*)

Data dependent (adaptive) weight

minimum-variance beamformer

$$\min_{\boldsymbol{w}} \boldsymbol{w}^T \boldsymbol{D}\boldsymbol{w} \text{ subject to } \boldsymbol{w}^T \boldsymbol{l}(\boldsymbol{r},\boldsymbol{\eta}) = 1$$

$$\Downarrow$$

$$\boldsymbol{w}^T(\boldsymbol{r},\boldsymbol{\eta}) = \frac{\boldsymbol{l}^T(\boldsymbol{r},\boldsymbol{\eta})\boldsymbol{D}^{-1}}{\boldsymbol{l}^T(\boldsymbol{r},\boldsymbol{\eta})\boldsymbol{D}^{-1}\boldsymbol{l}(\boldsymbol{r},\boldsymbol{\eta})} \text{ and } \hat{s}(\boldsymbol{r},\boldsymbol{\eta}) = \frac{\boldsymbol{l}^T(\boldsymbol{r},\boldsymbol{\eta})\boldsymbol{D}^{-1}\boldsymbol{b}}{\boldsymbol{l}^T(\boldsymbol{r},\boldsymbol{\eta})\boldsymbol{D}^{-1}\boldsymbol{l}(\boldsymbol{r},\boldsymbol{\eta})}$$

$$\|$$

$$\boldsymbol{L}(\boldsymbol{r})\boldsymbol{\eta} \leftarrow$$ beamformer pointing orientation

Generalized Wiener estimate:

$$\hat{\boldsymbol{s}}_N = \boldsymbol{R}\boldsymbol{L}_N^T(\boldsymbol{L}_N\boldsymbol{R}\boldsymbol{L}_N^T + \boldsymbol{C})^{-1}\boldsymbol{b}$$

⇑ source covariance matrix ⇑ noise covariance matrix

Use $\boldsymbol{R} \approx \boldsymbol{I}$, and $\boldsymbol{C} \approx g\,\boldsymbol{I}$ (assume no prior-information)

⇓

$$\hat{\boldsymbol{s}}_N = \boldsymbol{L}_N^T(\boldsymbol{L}_N\boldsymbol{L}_N^T + g\,\boldsymbol{I})^{-1}\boldsymbol{b}$$

minimum-norm estimate

Generalized Wiener estimate:

$$\hat{\boldsymbol{s}}_N = \boldsymbol{R}\boldsymbol{L}_N^T(\boldsymbol{L}_N\boldsymbol{R}\boldsymbol{L}_N^T + \boldsymbol{C})^{-1}\boldsymbol{b}$$

- use $\boldsymbol{D}=\boldsymbol{L}_N\boldsymbol{R}\boldsymbol{L}_N^T + \boldsymbol{C}$, and
- assume off-diagonals of $\boldsymbol{R}$ are all zero

$$\Downarrow$$

$$\hat{s}_p = R_{pp} l_P^T \boldsymbol{D}^{-1}\boldsymbol{b}$$

Relashonship, $\hat{s}_p^2 = R_{pp}$ leads to $R_{pp} = 1/(l_P^T \boldsymbol{D}^{-1} l_p)$

$$\underline{\hat{s}_p = (l_P^T \boldsymbol{D}^{-1}\boldsymbol{b})/(l_P^T \boldsymbol{D}^{-1} l_p)}$$

minimum-variance estimate

Problems when applying MV beamformer to MEG source localization

(1) How to determine beamformer orientation $\boldsymbol{\eta}$.

(2) $\|\boldsymbol{L}(\boldsymbol{r})\|$ – norm artifact.

(3) Output SNR degradation due to the matrix inversion.

How to determine beamformer orientation $\boldsymbol{\eta}$?

The weight $\boldsymbol{w}(\boldsymbol{r},h)$ is calculated for $\boldsymbol{r}$ and h.

- search all directions (Robinson and Vrba).
- use the MUSIC algorithm to determine $\boldsymbol{\eta}$ (Sekihara *et al.*).
- use vector beamformer formulation.
  (Spencer *et al.*.Van Veen *et al.*)

What happens if the beamformer orientation is different from the source orientation?

⇓

Severe signal-intensity loss

Computer simulation for calculating beamformer angular response

37-channel sensor array

A single source exists 6-cm below the sensor array

beamformer orientation different from the source orientation with $\delta\theta$

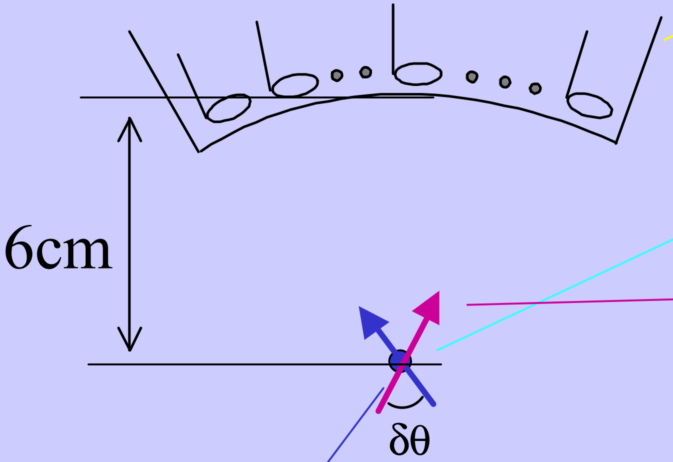

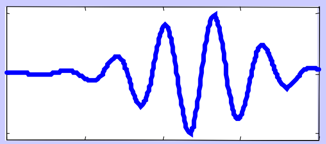

assumed source waveform

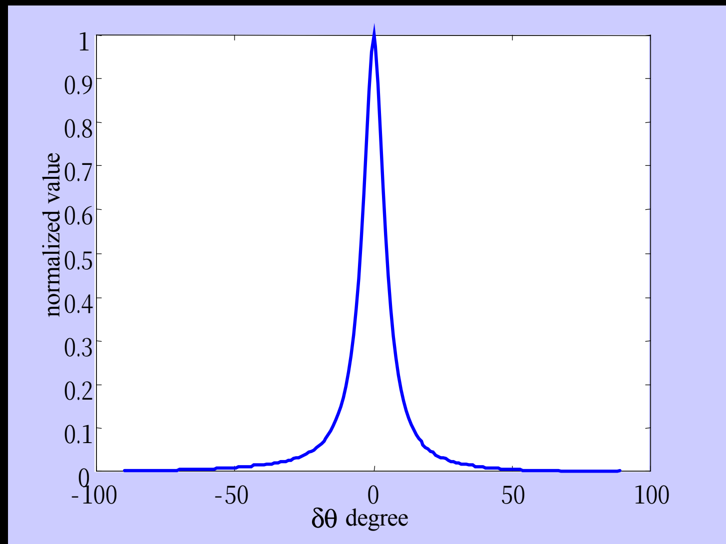

Calculated angular response

A single source exist at $\boldsymbol{r}$ with orientation $\boldsymbol{\eta}$ and time course $s(t)$

measured data: $\boldsymbol{b}(t) = [h_x \boldsymbol{l}_x(\boldsymbol{r}) + h_y \boldsymbol{l}_y(\boldsymbol{r}) + h_z \boldsymbol{l}_z(\boldsymbol{r})] s(t)$

When beamformer weight has a wrong orientation $\boldsymbol{\eta}'(\neq \boldsymbol{\eta})$

$$\boldsymbol{w}^T(\boldsymbol{r}, \boldsymbol{\eta}')\boldsymbol{b}(t) = \boldsymbol{w}^T(\boldsymbol{r}, \boldsymbol{\eta}')\underbrace{[h_x \boldsymbol{l}_x(\boldsymbol{r}) s(t) + h_y \boldsymbol{l}_y(\boldsymbol{r}) s(t) + h_z \boldsymbol{l}_z(\boldsymbol{r}) s(t)]}_{\Uparrow}$$

virtual three coherent sources

$$\approx 0$$

Vector beamformer formulation

Three weight vectors $[\boldsymbol{w}_x(\boldsymbol{r}), \boldsymbol{w}_y(\boldsymbol{r}), \boldsymbol{w}_z(\boldsymbol{r})]$ detects the *x*, *y*, and *z* component of the source moment, separately.

$$\min \boldsymbol{w}_x^T \boldsymbol{D} \boldsymbol{w}_x \text{ subject to } \boldsymbol{w}_x^T \boldsymbol{l}(\boldsymbol{r}, \boldsymbol{f}_x) = 1,\ \boldsymbol{w}_x^T \boldsymbol{l}(\boldsymbol{r}, \boldsymbol{f}_y) = 0,\ \boldsymbol{w}_x^T \boldsymbol{l}(\boldsymbol{r}, \boldsymbol{f}_z) = 0$$

$$\min \boldsymbol{w}_y^T \boldsymbol{D} \boldsymbol{w}_y \text{ subject to } \boldsymbol{w}_y^T \boldsymbol{l}(\boldsymbol{r}, \boldsymbol{f}_x) = 0,\ \boldsymbol{w}_y^T \boldsymbol{l}(\boldsymbol{r}, \boldsymbol{f}_y) = 1,\ \boldsymbol{w}_y^T \boldsymbol{l}(\boldsymbol{r}, \boldsymbol{f}_z) = 0$$

$$\min \boldsymbol{w}_z^T \boldsymbol{D} \boldsymbol{w}_z \text{ subject to } \boldsymbol{w}_z^T \boldsymbol{l}(\boldsymbol{r}, \boldsymbol{f}_x) = 0,\ \boldsymbol{w}_z^T \boldsymbol{l}(\boldsymbol{r}, \boldsymbol{f}_y) = 0,\ \boldsymbol{w}_z^T \boldsymbol{l}(\boldsymbol{r}, \boldsymbol{f}_z) = 1$$

$$\Downarrow$$

$$[\boldsymbol{w}_x(\boldsymbol{r}), \boldsymbol{w}_y(\boldsymbol{r}), \boldsymbol{w}_z(\boldsymbol{r})] = \boldsymbol{D}^{-1} \boldsymbol{L}(\boldsymbol{r}) [\boldsymbol{L}^T(\boldsymbol{r}) \boldsymbol{D}^{-1} \boldsymbol{L}(\boldsymbol{r})]^{-1}$$

and

$$\hat{\boldsymbol{s}}(t) = [\boldsymbol{L}^T(\boldsymbol{r}) \boldsymbol{D}^{-1} \boldsymbol{L}(\boldsymbol{r})]^{-1} \boldsymbol{L}^T(\boldsymbol{r}) \boldsymbol{D}^{-1} \boldsymbol{b}(t)$$

$\boldsymbol{f}_x = [1, 0, 0]^T,\ \boldsymbol{f}_y = [0, 1, 0]^T,\ \boldsymbol{f}_z = [0, 0, 1]^T$

Calculated beamformer angular response

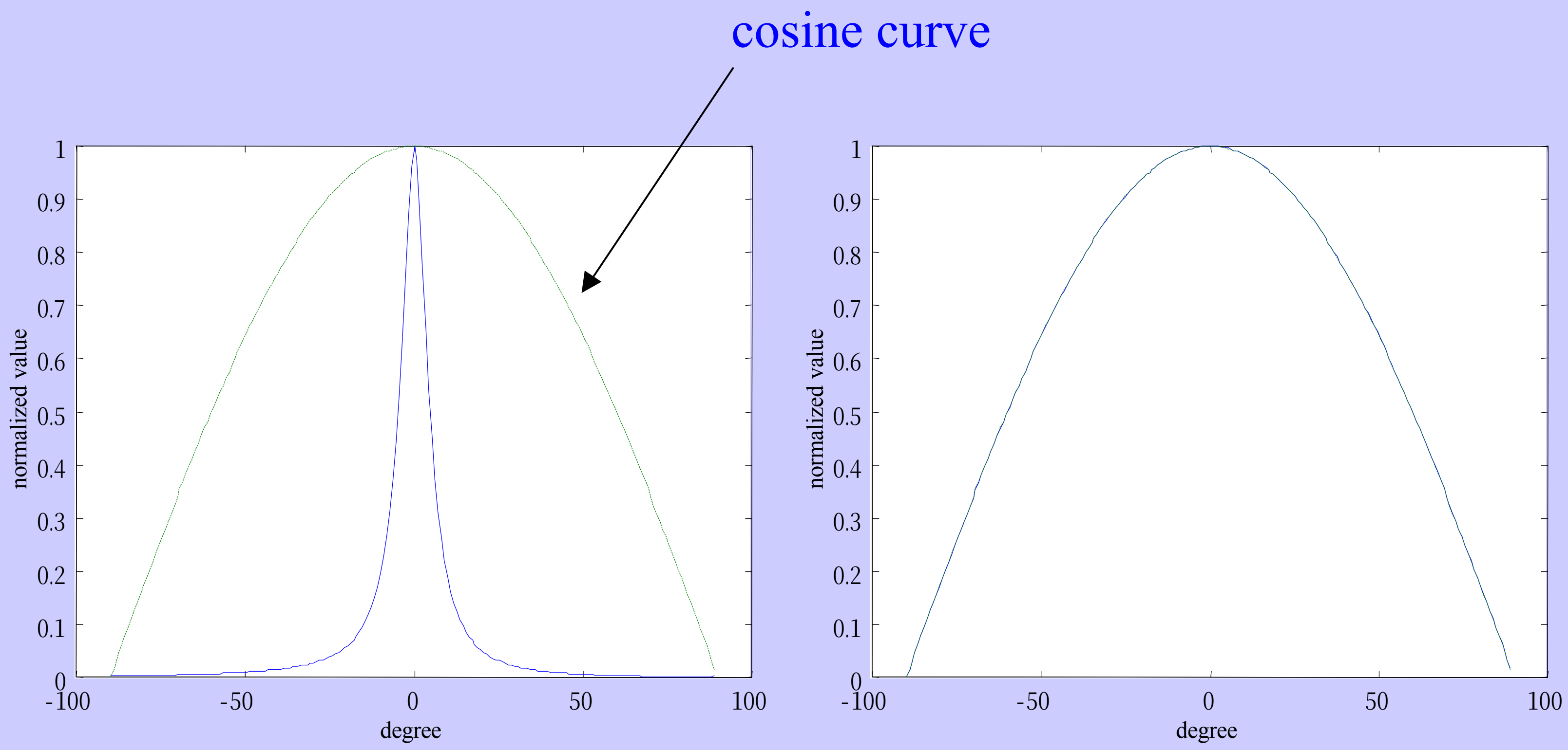

scalar beamformer

vector beamformer

$\|\boldsymbol{L}(\boldsymbol{r})\|$ – norm artifact

Severe artifacts arise near the center of the sphere, when the spherical conductor model is used.

To avoid these artifacts

- use normalized lead field (Van Veen *et al.*)
- use normalized weight (Robinson *et al.*, Sekihara *et al.*)

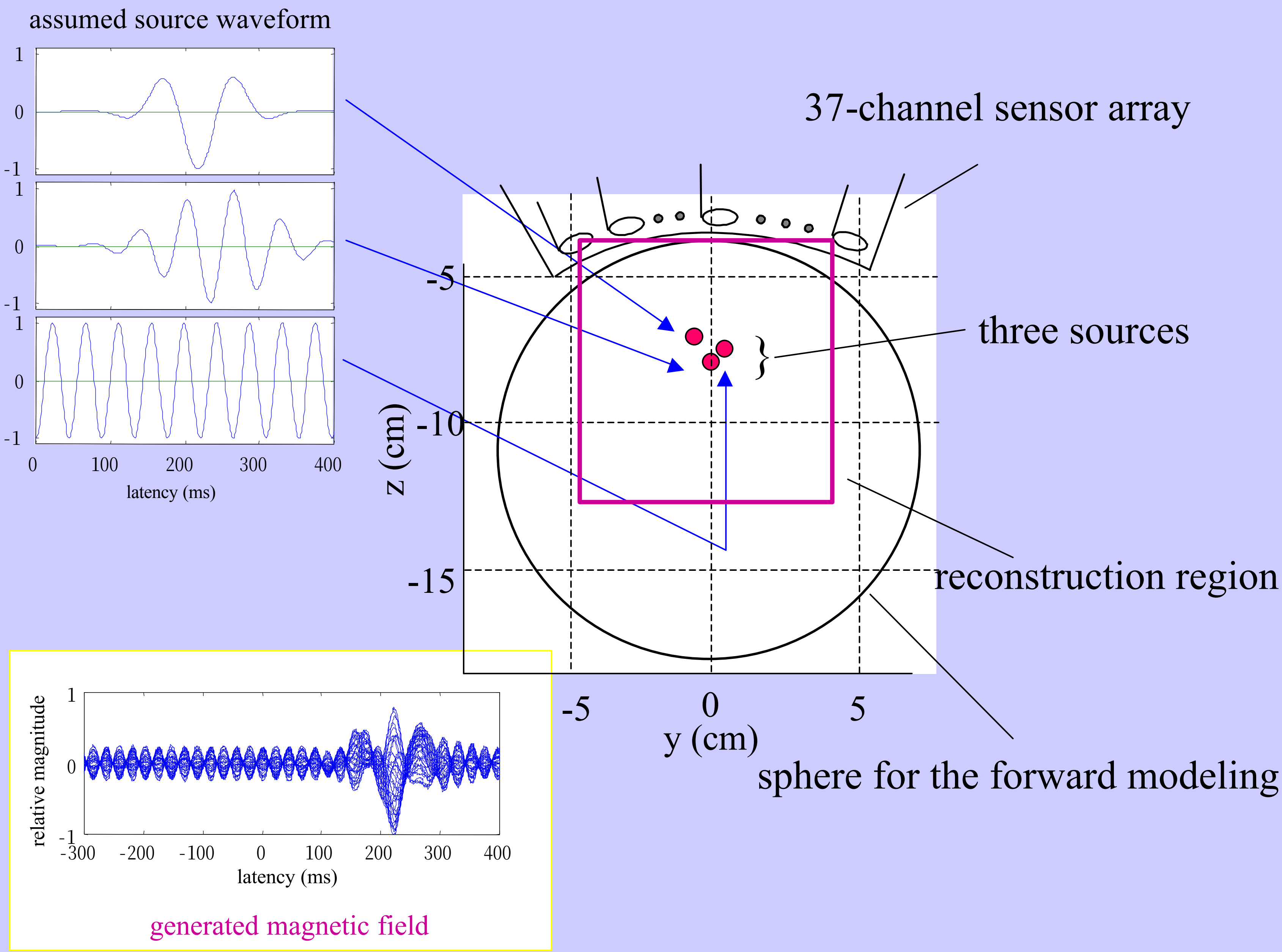

assumed source waveform
1
0
-1
0
100
200
300
400
latency (ms)
37-channel sensor array
three sources
-5
-10
-15
z (cm)
-5
0
5
y (cm)
reconstruction region
sphere for the forward modeling
relative magnitude
-300
-200
-100
latency (ms)
generated magnetic field

Time-averaged reconstruction $\left\langle \left\| \hat{\boldsymbol{s}}(\boldsymbol{r}, t) \right\|^2 \right\rangle$

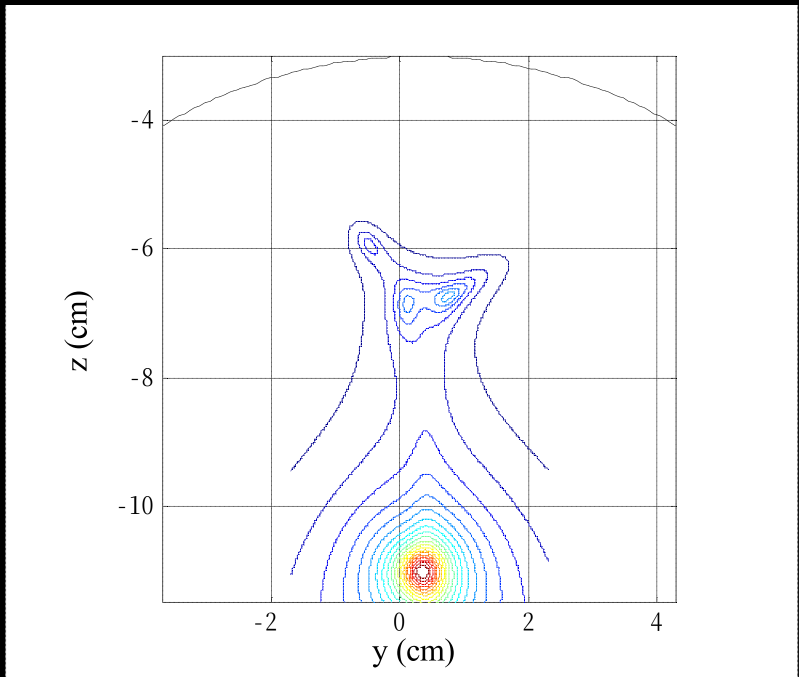

no normalization

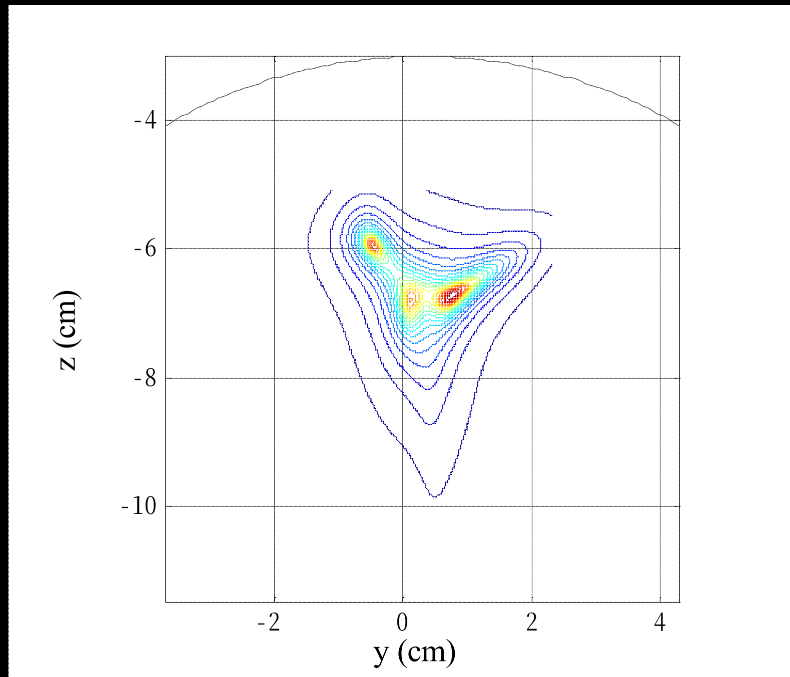

normalized lead field used

Borgiotti-Kaplan beamformer

$$\min_{\boldsymbol{w}} \boldsymbol{w}^T \boldsymbol{D} \boldsymbol{w} \text{ subject to } \boldsymbol{w}^T \boldsymbol{w} = 1$$

$$\Downarrow$$

$$\boldsymbol{w}^T(\boldsymbol{r},\boldsymbol{\eta}) = \frac{\boldsymbol{l}^T(\boldsymbol{r},\boldsymbol{\eta})\boldsymbol{D}^{-1}}{\sqrt{\boldsymbol{l}^T(\boldsymbol{r},\boldsymbol{\eta})\boldsymbol{D}^{-2}\boldsymbol{l}(\boldsymbol{r},\boldsymbol{\eta})}}$$

and

$$\left\langle \left\| \hat{\boldsymbol{s}}(\boldsymbol{r},\boldsymbol{\eta}) \right\|^2 \right\rangle = \frac{\boldsymbol{l}^T(\boldsymbol{r},\boldsymbol{\eta})\boldsymbol{D}^{-1}\boldsymbol{l}(\boldsymbol{r},\boldsymbol{\eta})}{\boldsymbol{l}^T(\boldsymbol{r},\boldsymbol{\eta})\boldsymbol{D}^{-2}\boldsymbol{l}(\boldsymbol{r},\boldsymbol{\eta})}$$

Vector extension of Borgiotti-Kaplan beamformer

$$\min \boldsymbol{w}_x^T \boldsymbol{D} \boldsymbol{w}_x \text{ subject to } \boldsymbol{w}_x^T \boldsymbol{w}_x = 1,\ \boldsymbol{w}_x^T \boldsymbol{l}(\boldsymbol{r}, \boldsymbol{f}_y) = 0,\ \boldsymbol{w}_x^T \boldsymbol{l}(\boldsymbol{r}, \boldsymbol{f}_z) = 0$$

$$\min \boldsymbol{w}_y^T \boldsymbol{D} \boldsymbol{w}_y \text{ subject to } \boldsymbol{w}_y^T \boldsymbol{l}(\boldsymbol{r}, \boldsymbol{f}_x) = 0,\ \boldsymbol{w}_y^T \boldsymbol{w}_y = 1,\ \boldsymbol{w}_y^T \boldsymbol{l}(\boldsymbol{r}, \boldsymbol{f}_z) = 0$$

$$\min \boldsymbol{w}_z^T \boldsymbol{D} \boldsymbol{w}_z \text{ subject to } \boldsymbol{w}_z^T \boldsymbol{l}(\boldsymbol{r}, \boldsymbol{f}_x) = 0,\ \boldsymbol{w}_z^T \boldsymbol{l}(\boldsymbol{r}, \boldsymbol{f}_y) = 0,\ \boldsymbol{w}_z^T \boldsymbol{w}_z = 1$$

$$\Downarrow$$

let $\mu = x,\ y$ or z

$$\boldsymbol{w}_\mu(\boldsymbol{r}) = \frac{\boldsymbol{D}^{-1}\boldsymbol{L}(\boldsymbol{r})[\boldsymbol{L}^T(\boldsymbol{r})\boldsymbol{D}^{-1}\boldsymbol{L}(\boldsymbol{r})]^{-1}\boldsymbol{f}_\mu}{\sqrt{\boldsymbol{f}_\mu^T \boldsymbol{\Omega} \boldsymbol{f}_\mu}}$$

$$W = [\boldsymbol{L}^T(\boldsymbol{r})\boldsymbol{D}^{-1}\boldsymbol{L}(\boldsymbol{r})]^{-1}\boldsymbol{L}^T(\boldsymbol{r})\boldsymbol{D}^{-2}\boldsymbol{L}(\boldsymbol{r})[\boldsymbol{L}^T(\boldsymbol{r})\boldsymbol{D}^{-1}\boldsymbol{L}(\boldsymbol{r})]^{-1}$$

Time-averaged reconstruction $\left\langle \|\hat{\boldsymbol{s}}(\boldsymbol{r},t)\|^2 \right\rangle$

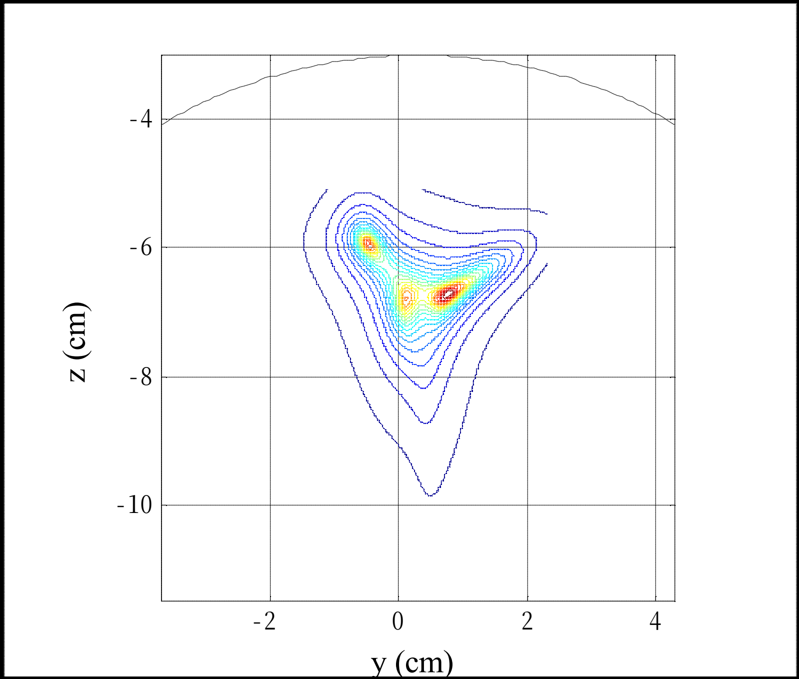

normalized lead field used

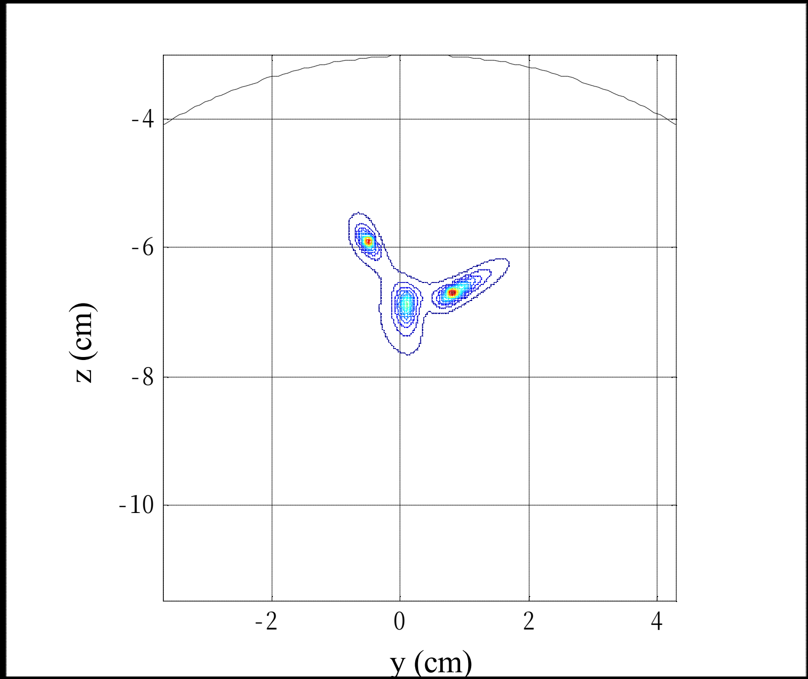

normalized weight used
(B-K beamformer results)

Resolution kernel for BK beamformer

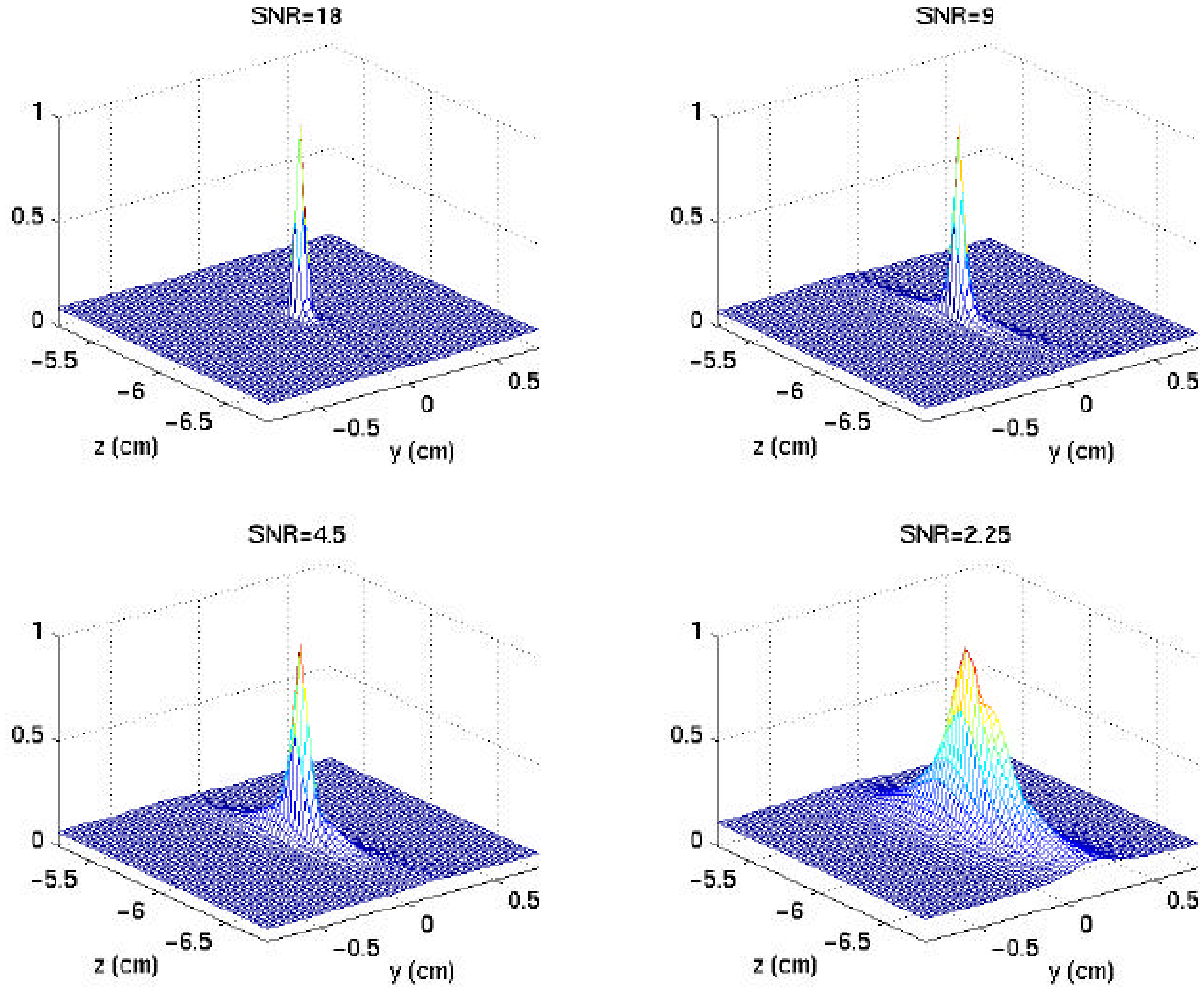

Output SNR degradation for spatio-temporal reconstruction

Signal-to-noise ratio of the beamformer output is severely degraded even by a small error in the estimated lead field

This is caused by the use of direct matrix inversion

To avoid this,

- use regularized inverse (Robinson *et al*.)
- use eigenspace projection (Sekihara *et al*.)

Eigenspace projection

Eigendecomposition of $\boldsymbol{D}$

$$\boldsymbol{D} = \boldsymbol{U}\left[\begin{array}{ccc|cc} \lambda_1 & 0 & \cdots & \cdot & 0 \\ 0 & \ddots & & 0 & \cdot \\ \vdots & & \lambda_P & & \vdots \\ \hline \cdot & 0 & & \ddots & 0 \\ 0 & \cdot & \cdots & 0 & \lambda_M \end{array}\right]\boldsymbol{U}^T = \boldsymbol{U}\begin{bmatrix} \boldsymbol{\Lambda}_S & 0 \\ 0 & \boldsymbol{\Lambda}_N \end{bmatrix}\boldsymbol{U}^T$$

$$\boldsymbol{U} = [\underbrace{\boldsymbol{e}_1, \ldots, \boldsymbol{e}_P}_{\boldsymbol{E}_S} \mid \underbrace{\boldsymbol{e}_{P+1}, \ldots, \boldsymbol{e}_M}_{\boldsymbol{E}_N}] = [\boldsymbol{E}_S \mid \boldsymbol{E}_N]$$

Extension to eigenspace projection beamformer

$$\bar{\boldsymbol{w}}_\mu = \boldsymbol{E}_S \boldsymbol{E}_S^T \boldsymbol{w}_\mu, \quad \text{where } \mu = x, y \text{ or } z$$

SNR consideration

Output of eigenspace-projected BK beamformer

$$\propto \frac{[\boldsymbol{l}^T(\boldsymbol{r})\boldsymbol{\Gamma}_S \boldsymbol{l}(\boldsymbol{r})]^2}{[\boldsymbol{l}^T(\boldsymbol{r})\boldsymbol{\Gamma}_S^2 \boldsymbol{l}(\boldsymbol{r})]} \quad \text{where } \boldsymbol{\Gamma}_S = \boldsymbol{E}_S \boldsymbol{\Lambda}_S^{-1} \boldsymbol{E}_S^T, \quad \boldsymbol{\Gamma}_N = \boldsymbol{E}_N \boldsymbol{\Lambda}_N^{-1} \boldsymbol{E}_N^T$$

Output of BK beamformer

$$\propto \frac{[\boldsymbol{l}^T(\boldsymbol{r})\boldsymbol{\Gamma}_S \boldsymbol{l}(\boldsymbol{r})]^2}{[\boldsymbol{l}^T(\boldsymbol{r})\boldsymbol{\Gamma}_S^2 \boldsymbol{l}(\boldsymbol{r}) + \boldsymbol{e}^T G_N^2 \boldsymbol{e}]}$$

overall error in estimating $\boldsymbol{l}(\boldsymbol{r})$

Even when $\boldsymbol{e}$ is small, $\boldsymbol{e}^T \boldsymbol{\Gamma}_N^2 \boldsymbol{e}$ may not be small

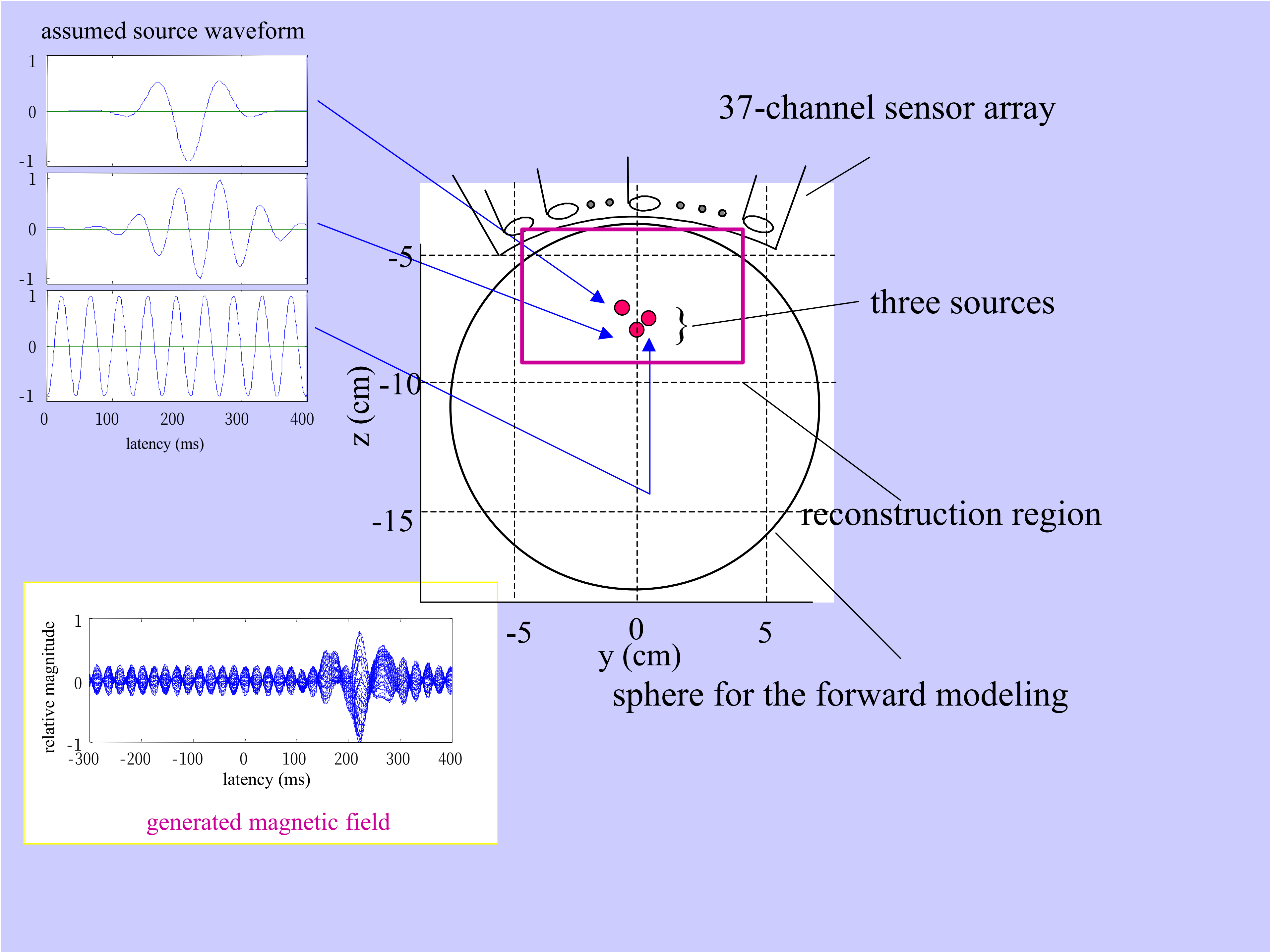

assumed source waveform
1
0
-1
0
100
200
300
400
latency (ms)
37-channel sensor array
three sources
z (cm)
-5
-10
-15
reconstruction region
-5
0
5
y (cm)
sphere for the forward modeling
relative magnitude
-300
-200
-100
latency (ms)
generated magnetic field

Spatio-tempotal reconstruction by vector-extended BK beamformer

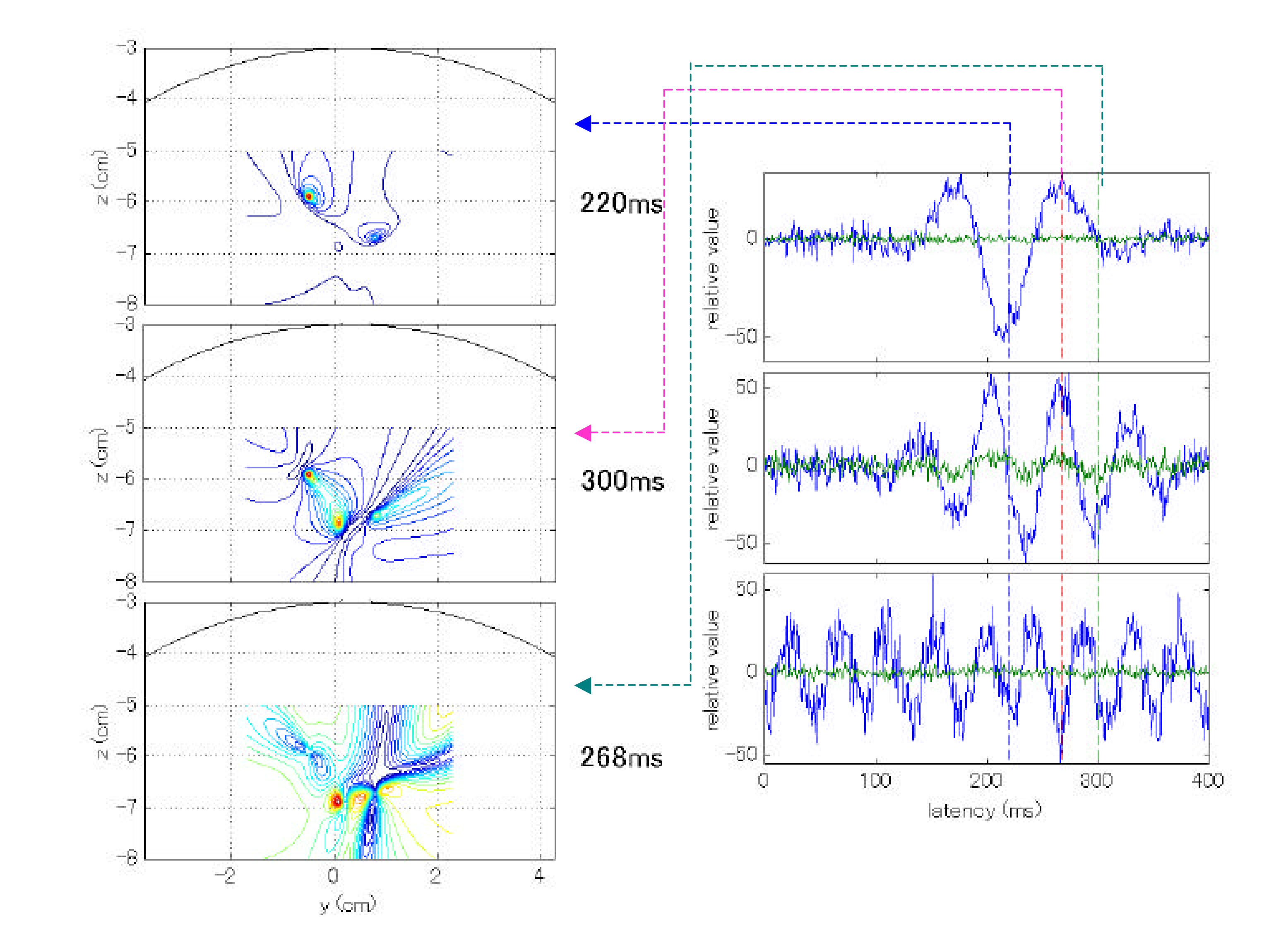

Spatio-tempotal reconstruction by vector-extended BK beamformer with regularized inverse, $(\boldsymbol{D} + g\,\boldsymbol{I})^{-1}$

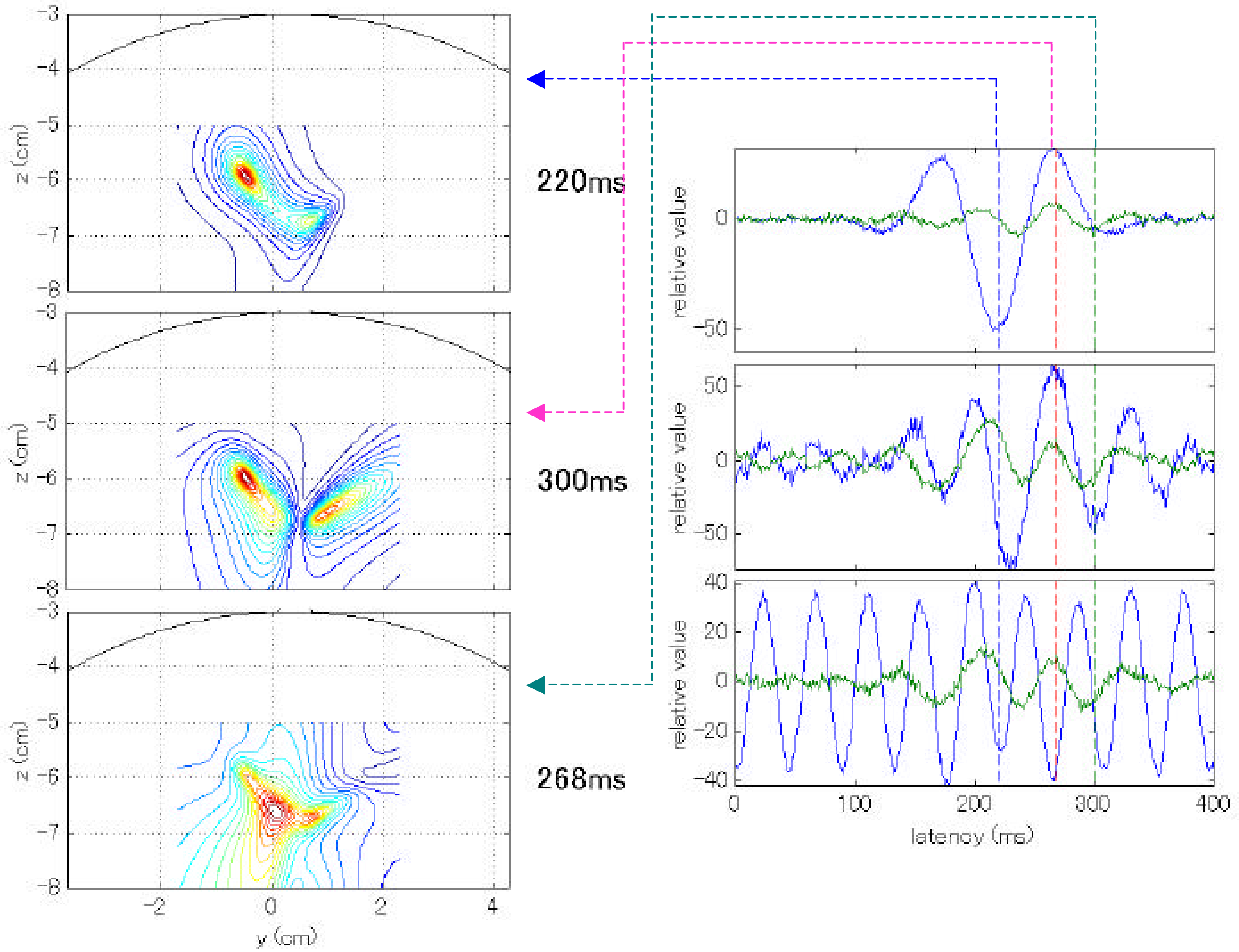

Spatio-tempotal reconstruction by vector-extended BK beamformer with eigen-space projection

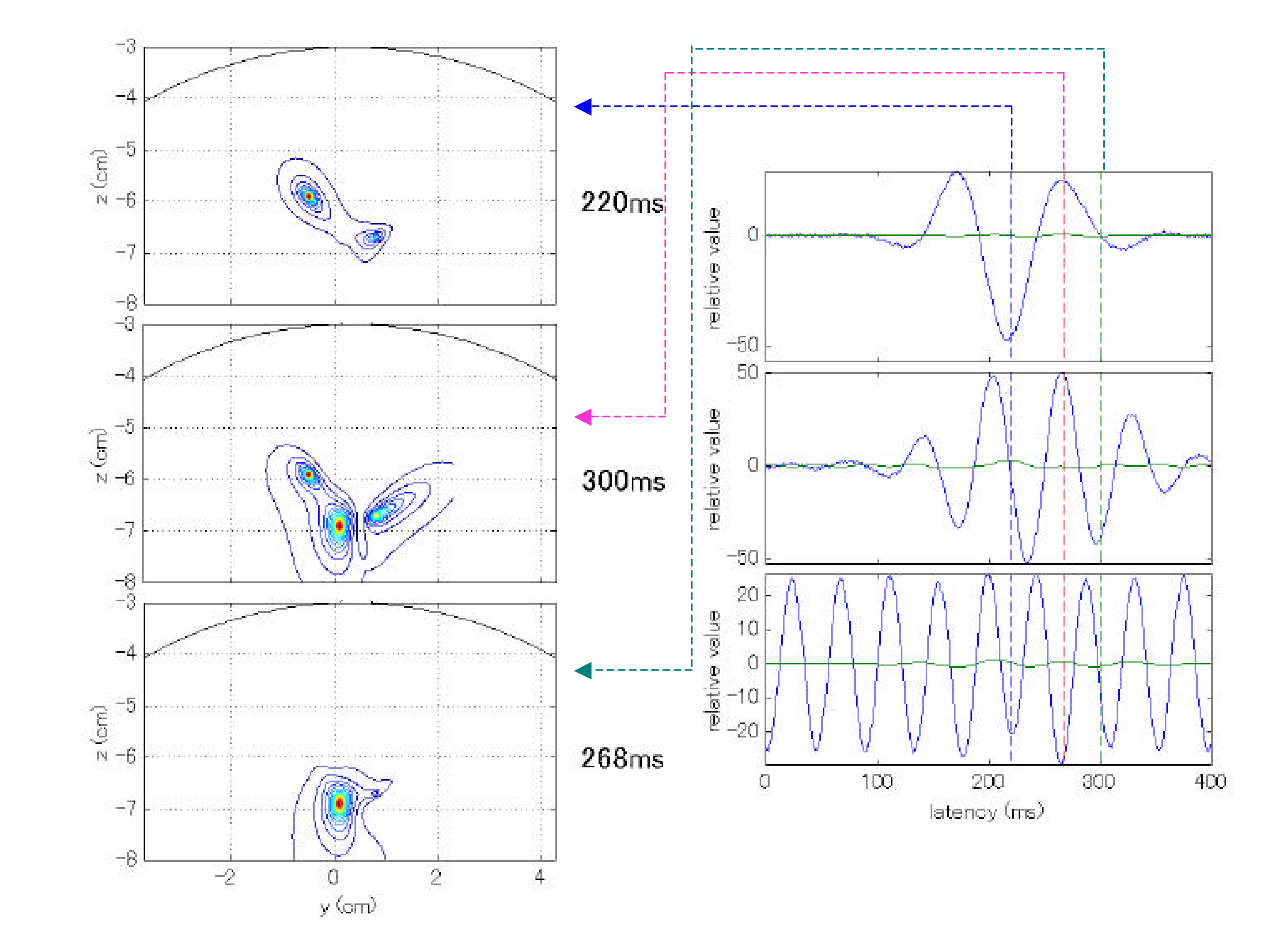

Eigen-space projection does not preserve the null constraints

That is,

$$\left[\boldsymbol{E}_S \boldsymbol{E}_S^T \boldsymbol{w}_x\right]^T \boldsymbol{l}_y(\boldsymbol{r}) \neq 0, \quad \left[\boldsymbol{E}_S \boldsymbol{E}_S^T \boldsymbol{w}_x\right]^T \boldsymbol{l}_z(\boldsymbol{r}) \neq 0,$$

$$\left[\boldsymbol{E}_S \boldsymbol{E}_S^T \boldsymbol{w}_y\right]^T \boldsymbol{l}_x(\boldsymbol{r}) \neq 0, \quad \left[\boldsymbol{E}_S \boldsymbol{E}_S^T \boldsymbol{w}_y\right]^T \boldsymbol{l}_z(\boldsymbol{r}) \neq 0,$$

$$\left[\boldsymbol{E}_S \boldsymbol{E}_S^T \boldsymbol{w}_z\right]^T \boldsymbol{l}_x(\boldsymbol{r}) \neq 0, \quad \left[\boldsymbol{E}_S \boldsymbol{E}_S^T \boldsymbol{w}_z\right]^T \boldsymbol{l}_y(\boldsymbol{r}) \neq 0.$$

This fact does not cause a problem.
(Poster: 167b)

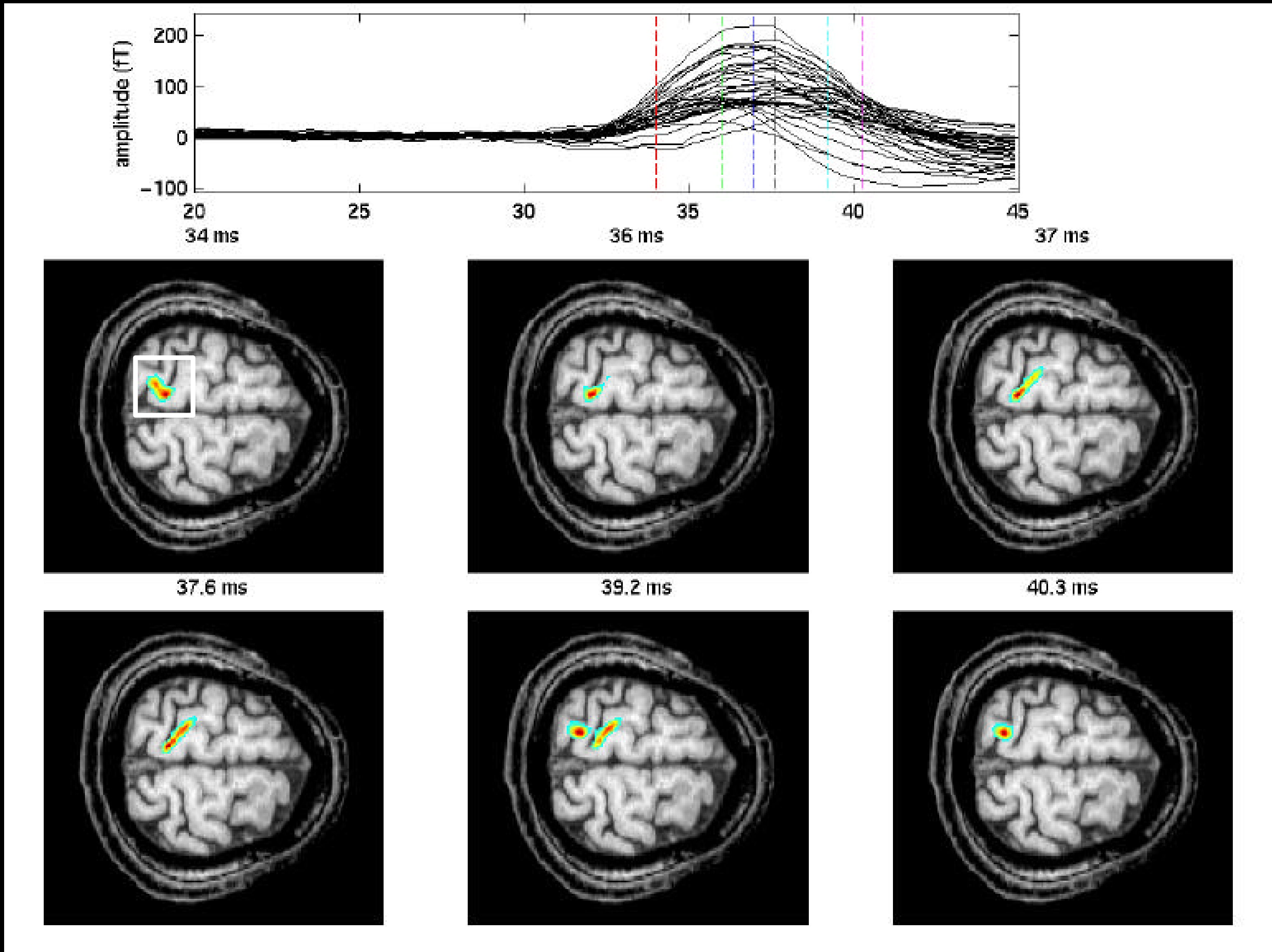

amplitude (fT)
200
100
0
−100
20
25
30
35
40
45
34 ms
36 ms
37 ms
37.6 ms
39.2 ms
40.3 ms

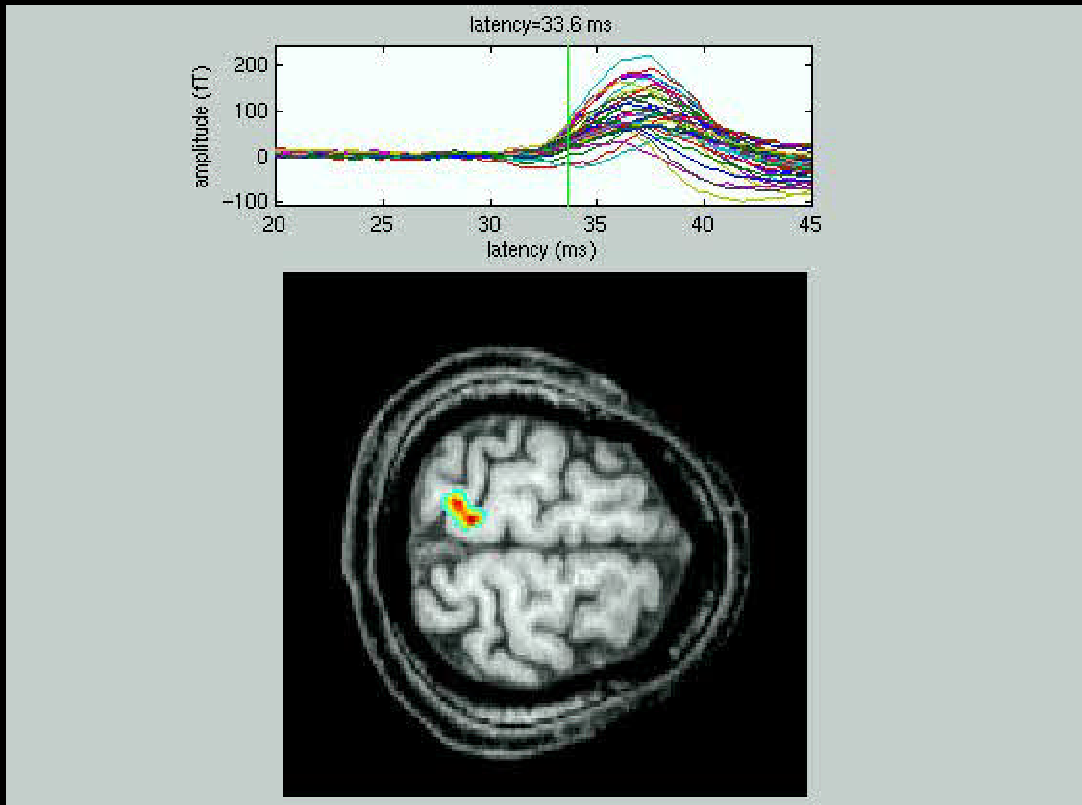
latency=33.6 ms
amplitude (fT)
200
100
0
−100
20
25
30
35
40
45
latency (ms)

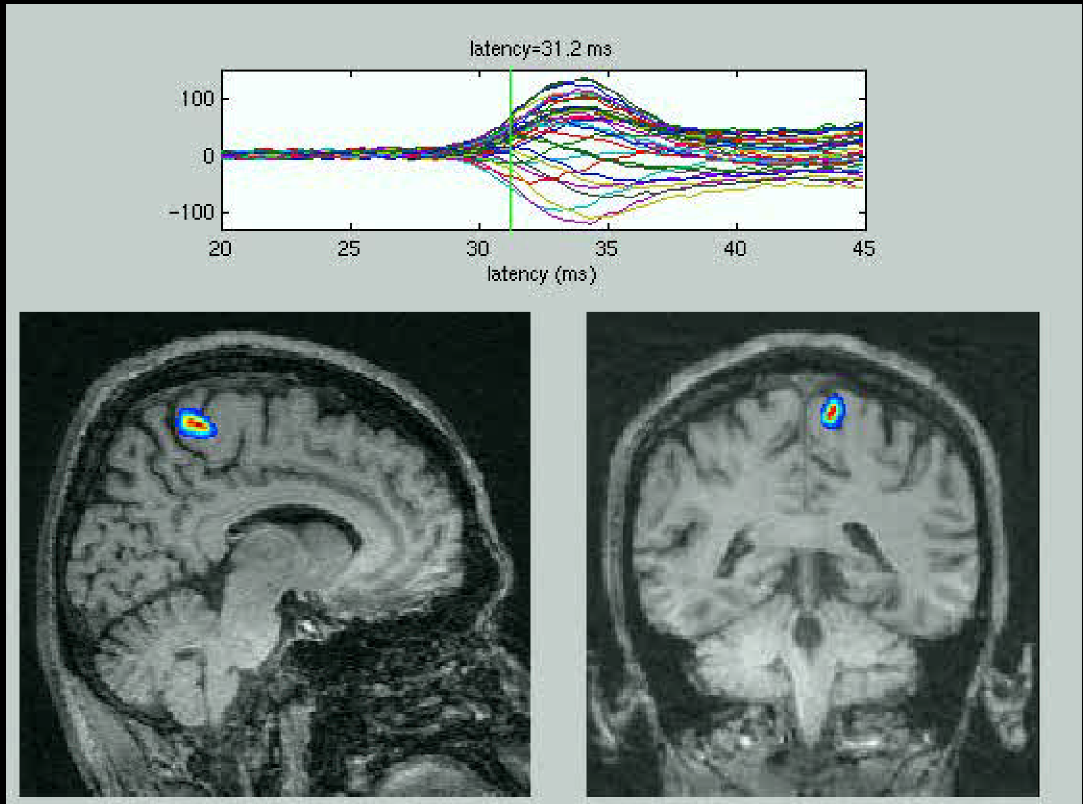
latency=31.2 ms
100
0
−100
20
25
30
35
40
45
latency (ms)

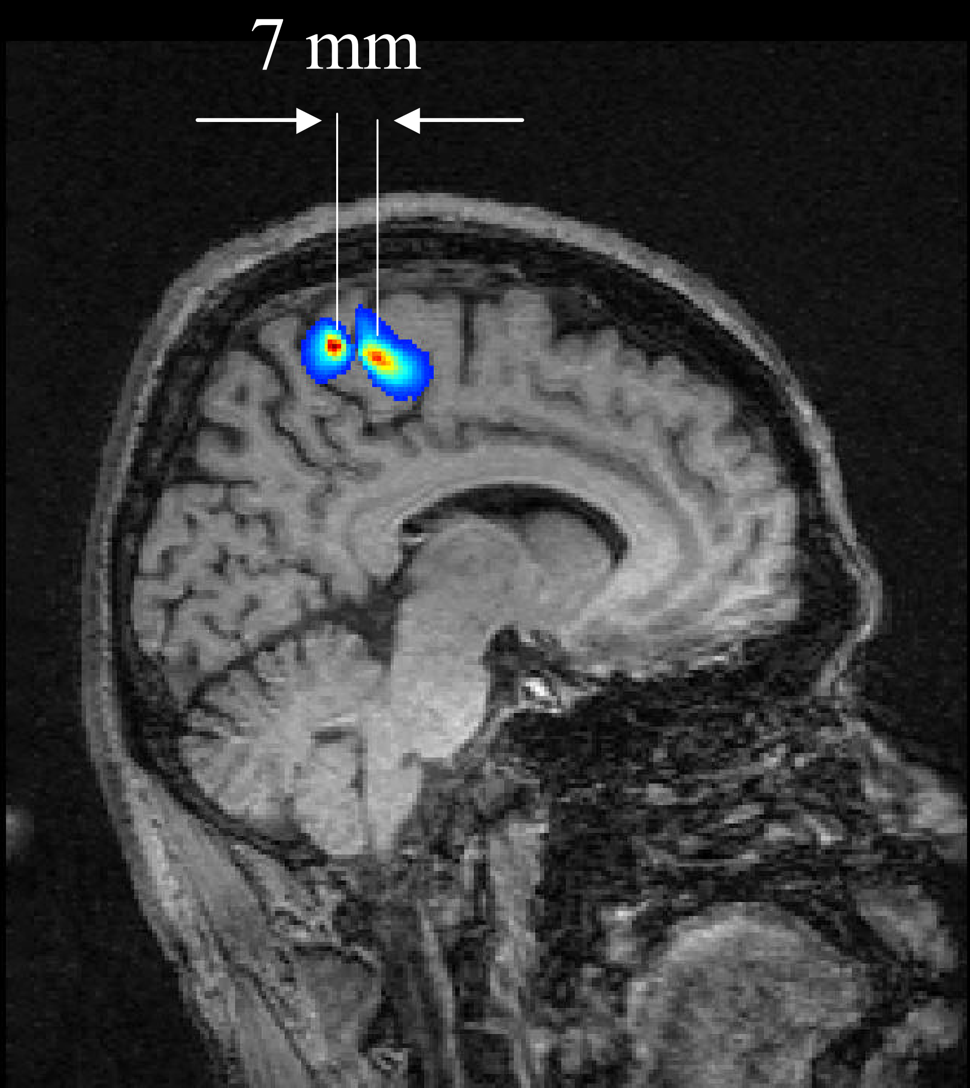

Poster: 92a

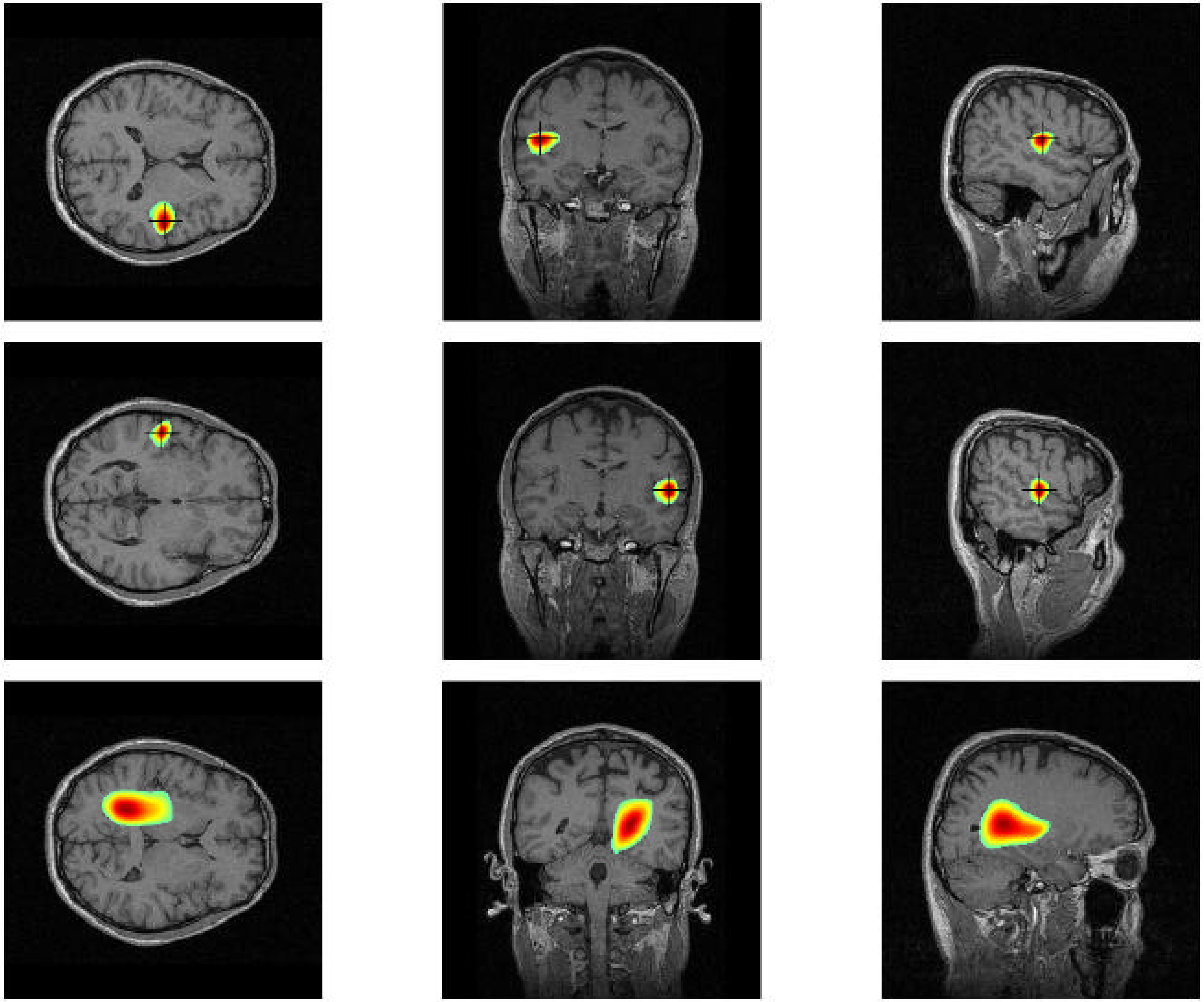

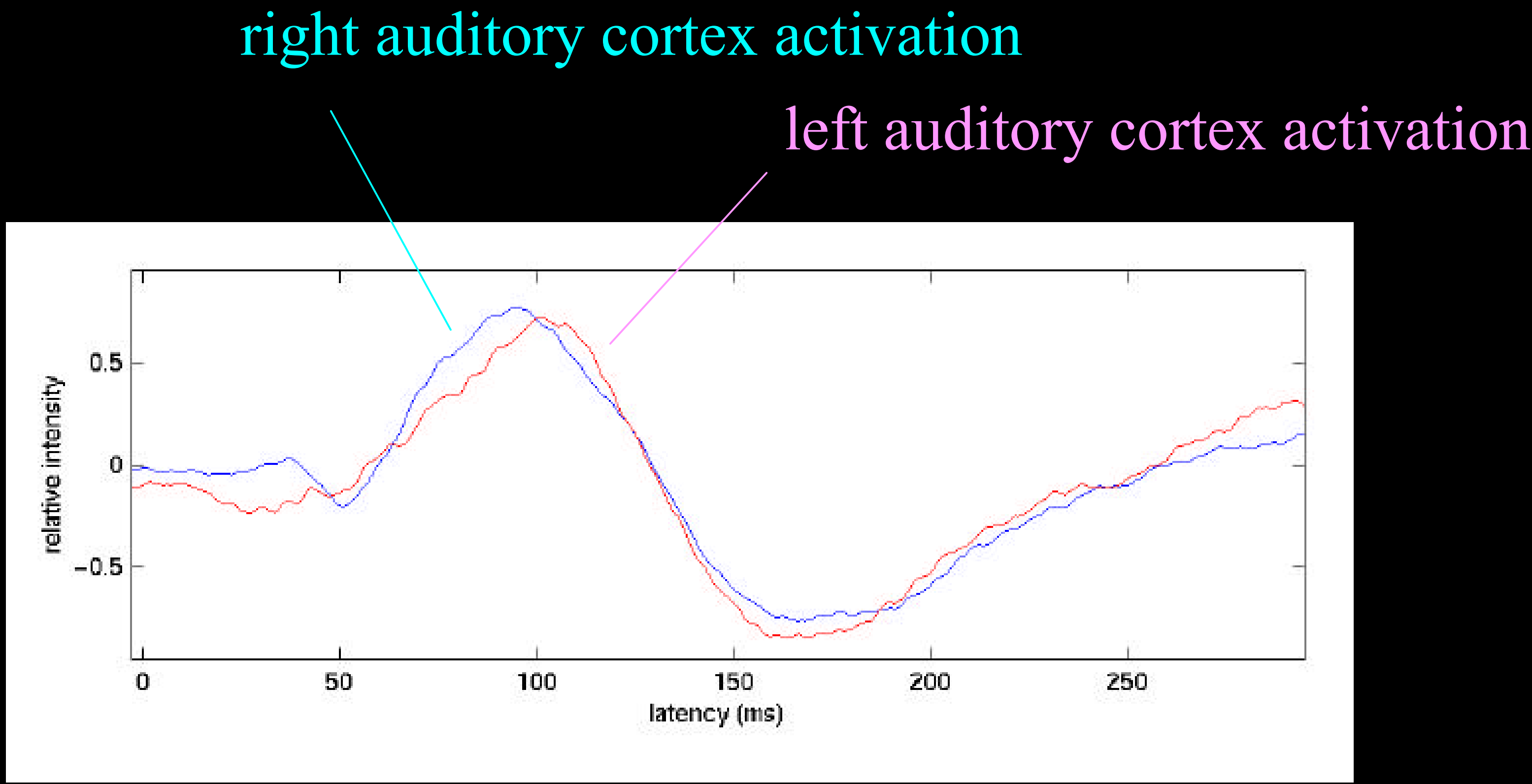

correlation coefficient: 0.97

Summary

- Adaptive spatial filter techniques can provide a spatial resolution higher than that of non adaptive techniques.

- This is because the spatial resolution for non-adaptive techniques is limited by the sensor configuration but adaptive techniques can exceed this limit.

- Correlated source activities, however, affect the quality of the results obtained by adaptive techniques.

Therefore

Adaptive techniques may be suited to observe relatively small cortical regions with high spatial resolution, and non-adaptive techniques may be suited to observe whole-brain activities.

Collaborators

Kanazawa Institute of Technology
Dr. Isao Hashimoto

Laboratory of Physiological Sciences
Dr. Keiji Sakuma

Communications Research Lab.
Dr. Touru Miyauchi

Communications Research Lab.
Dr. Norio Fujimaki

Siraume University
Dr. Ryosuke Takino

University of Utah
Dr. Srikantan S. Nagarajan

M. I. T.
Dr. Alec Marantz

University of Maryland
Dr. David Poeppel

University of California
Dr. Tim Roberts

University of Tokyo
Dr. Yasushi Miyashita